CHAPTER 5

Effect of New Extended Type Non-rectangular PCM Enclosure on Thermo-electric Performance of PV/PCM Systems

An innovative concept of extended non-rectangular phase change material (PCM) enclosure integrated with a photovoltaic (PV) panel has been investigated in this chapter that manifests 7.26 times incoming solar radiation than the simple PV system. The strategic distribution of PCM is achieved by controlling certain geometric parameters such as lower thickness ratio, extension ratio and profile of right wall. With optimization of these parameters, the span of convection dominated regime is prolonged to more than 120 minutes which conceded 20.5% more melting compared to the conventional rectangular design of same PCM volume. Electric conversion efficiency can approach to 96.37% of its rated value with the application of strategies demonstrated in the chapter. Moreover, incoming radiation absorbing capacity can approach to 67.35% for recommended configuration. An experimentally validated numerical model is used to report the findings of this investigation which can predict exact melting morphology and thermal behavior of the system. This chapter provides useful information that will be helpful in developing more efficient PV techniques that can meet the ever rising global energy demands.

5.1 Introduction

Exponential population growth during late 20th century and early 21st century leads to uncontrolled pollution and global warming problems due to excessive consumption of fossil fuels to meet growing energy demands [1, 2, 79]. Increasing the dependency on renewable energy resources such as solar energy is one of the remedies to produce pollution free and clean energy [80, 81]. Photovoltaic (PV) technology has great potential of harnessing solar energy in form of

high grade energy (electric current) to balance these growing global energy demands [82, 83]. However, lot of incoming radiation is being wasted in form of low grade energy (wasted heat) owing to its low electrical conversion efficiency. High waste heat production further degrades its electric conversion performance by elevating the temperature of PV panel [10, 40]. The performance of PV panel bears an inverse relationship with its operating temperature i.e electric conversion performance is degraded with rise in operating temperature. Hussain et al., [10] reported a decrease of 0.5% in electric conversion efficiency with per degree rise of PV panel temperature. Moreover, a declination rate of 0.65%°C in electric current yield and 0.08%°C in electric conversion efficiency is being reported by Radziemska and Klugmann [40]. This waste heat production makes it a challenging technological hitch for the scientific community to enhance its operational efficiency. Waste heat management techniques involve thermal regulation of PV panel by extracting waste heat by integrating some heat extraction or storage device without any hindrance in incoming solar radiation. Photovoltaic thermal (PV/T) systems [44, 47, 84, 85], photovoltaic system integrated with phase change material (PV/PCM) [59, 86–88] and photovoltaic thermal system integrated with phase change material (PV/T-PCM) [5, 48, 89], are such commonly exercised waste heat management techniques to improve the electric performance of PV panels. Additionally, exercising these strategies has maximized the utilization of the incoming radiation in form of electric power and extracted heat content.

PV/PCM systems have become center of attraction among researchers due to its high heat storing capacity of phase change material (PCM) and use of this stored heat during nocturnal hours for various applications. PV/PCM system enhances the performance of PV panel by absorbing heat as latent heat and making it work at lower temperature [75]. However, PV/PCM systems also have some limitations such as low thermal conductivity which results in slow melting and heat removal rates that degrades the efficiency of the system. Such limitations are generally abridged by either using fins within PCM enclosure [50, 51] or by enhancing its thermo-physical properties such as adding nano-additives [54, 57, 58] to PCM. Some researchers focused on the importance of convective melting of PCM on the performance of PV/PCM system. Ezan et al., [36] stated that higher melting rates are observed in convective melting compared to conductive melting. Further Jany and Bejan, [38] explained all four regimes of melting for a rectangular enclosure and stated that melting rates declines in solid-shrinking regime of melting.

Moreover, some researchers focused on on enhancing the performance of PV/PCM system by increasing the duration of quasi-steady convection regime and decreasing the span of solid-shrinking regime by modification in designs of PCM enclosures. Akshayveer et al., [39] found that declined melting rates during solid-shrinking regime for rectangular enclosure cause an adverse effect on performance of PV panel. They suggested different type of non-rectangular enclosures to enhance the performance of PV panel by promoting convective melting and minimizing the duration of solid-shrinking regime. However, compactness of the system is compensated in order to maintain same volume of PCM with in the enclosure. Further Rabie et al., [55]

proposed the use of extended rectangular PCM enclosure in order to make more PCM available for convection dominated melting. They tested different over-height ratio of 0-60% and found that a better temperature uniformity is maintained in extended PCM enclosure. However, the distance between PV layer and right wall of PCM is reduced that decreases the melting rates and performance of PV/PCM system in spite of connective melting of PCM in the extended part of enclosure at high over-height ratio.

From the above discussion, it is evident that (1) thermo-electric performance of PV/PCM system is enhanced by design modification of PCM enclosure, (2) scientific community made regular efforts to upgrade PCM enclosure designs, and (3) melting front morphology plays an important role in designing the extended PCM enclosure. Hence, non-rectangular extended PCM enclosures are desirable to maintain convection dominated melting in both extended as well as aligned part to PV panel for maximum duration. Further, extended height must be optimized for same volume of PCM in order to get better thermo-electric performance and compactness of the system. Considering the higher operating temperature of PV panel, the intention of this paper is to provide a well optimized PCM enclosure design that enhances convection dominated melting and performance of PV/PCM system. This new concept of non-rectangular extended PCM enclosure has shown significant system performance enhanced which has been discussed in the following sections.

The primary objective of the study is to enhance thermo-electric performance of the PV/PCM system. This objective is achieved by extending convection dominated melting (quasi-steady convection regime) and allow more PCM available in top aligned part as well as extended part of the PCM enclosure. New enclosure designs (non-rectangular extended enclosure) are conceptualized as shown in Figure 5.1(b) which are the extension to simple non-rectangular designs ($H_e = 0$). The right wall (opposite to PV panel) profile of enclosure is ruled by equation of $y = (ax - b)^{1/n}$, where the exponent 'n' decides the shape of profile ($n = 1$ for linear profile, and $n = 2$ and 3 for parabolic and cubic profile respectively). The constants 'a' and 'b' are adjusted to keep the same volume of enclosure as of rectangular one (Figure 5.1(a)). Melting front extracts heat away from PV panel to the extended part as well as to top aligned part which is designed according to melting front morphology, hence extended quasi-steady convection regime is observed. However, increase in extended height will compensate the distance between PV panel and aligned right wall of enclosure that will affect the melting process adversely hence extended height must be optimized to further modify the design. Moreover, the lower thickness ratio (L_1/L) is another variable to improve the design of non-rectangular extended enclosure. Therefore, PCM enclosure is further modified by optimizing lower thickness ratio and getting a prolonged duration of quasi-convection regime and enhanced thermo-electric performance. Though there can be numerous shapes of extended part that can be analyzed, the reported shapes can be used as guidance for further research and development of efficient enclosure designs. PV/PCM system with different configurations of PCM enclosure is studied under same

boundary conditions with the help of an experimentally validated computational model. The natural convection dominated melting is affected by these various shapes of enclosure, hence thermo-electric performance is analyzed for improved designs. We hope that the findings of this paper will be helpful in further designing and developing better enclosure shapes that will assist better thermo-electric performances.

5.2 Solution methodology

5.2.1 Problem formulation

PV/PCM system is formulated as 2D numerical model to analyze its electric and heat storage performance under a given incident solar radiation (I_solar). Figure 5.1(a) shows the schematic diagram of PV/PCM system with rectangular PCM enclosure which contains three main regions namely glass (thickness t_g = 3 mm) PV cell (thicknesst_{pv} = 1 mm), and PCM enclosure (thickness L = 20 mm). The height of the system (H_{pv}) is considered 100 mm and PV/PCM system is categorized into four different geometric configuration based on the shape of PCM enclosure such as PV/PCM system with rectangular PCM enclosure is designated as type – A configuration. The PV/PCM system with non-rectangular PCM enclosure is categorized into three different configuration based on profile of right wall of enclosure. The general profile of right wall is $y = (ax - b)^{1/n}$ which is different in all configurations i.e linear profile (n = 1) is designation to type – B enclosure while parabolic and cubic (n = 2&3) are designation to type – C and D configurations respectively. The constants 'a' and 'b' are adjusted according to lower thickness ratio (L_1/L) and extension ratio (H_e/H_{pv}) so that volume of PCM remains same as of rectangular PCM enclosure.

Rubitherm RT27 is chosen as PCM for all type of configurations and thermo-physical properties of all materials used in different regions of system are listed in Table 2.2. Glass and PV cell region are modelled as solid with conductive heat transfer while PCM region is modelled as multiphase region in which solid PCM turns to liquid by absorbing latent heat. All the thermo-physical properties of PCM are considered as homogenous and invariable for the phase change process except density which is dependent on temperature according to Boussinesq approximation in liquid phase of material.

5.2.2 Boundary conditions

At top wall of glass region, incident solar radiation (I_{solar}) is balanced by conductive heat flux into the wall and total heat flux loss to the surroundings from the wall which comprises of convective (q''_{conv}) and radiative losses (q''_{rad}). The energy balance at top wall can be given by Eqs. 2.1-2.6.:

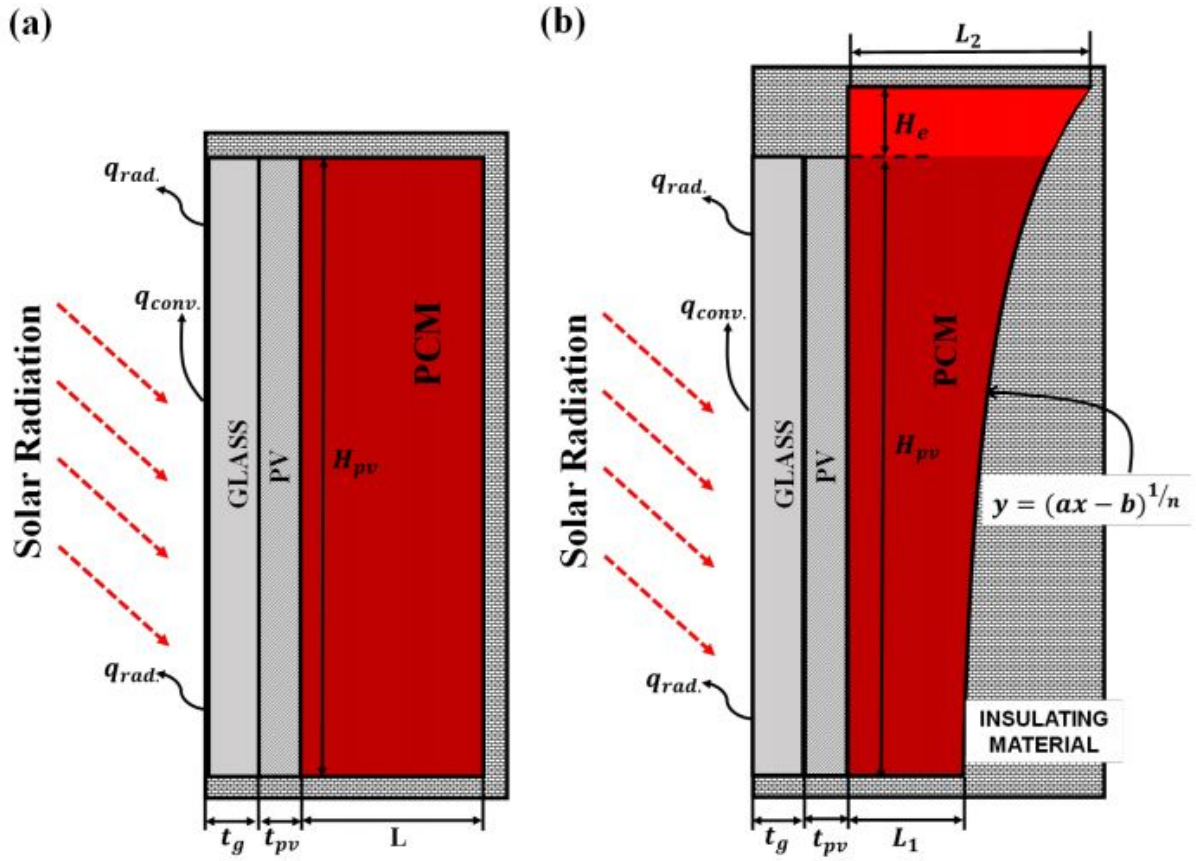

Figure 5.1: Two dimensional schematic diagram of PV/PCM systems (a) with rectangular PCM enclosure (Type – A), and (b) non-rectangular extended PCM enclosure with a general right wall profile, $y = (ax - b)^{(1/n)}$, $n = 1$ for type-B, $n = 2$ for type-C and $n = 3$ for type-D.

In all configurations of PV/PCM system, all outside boundaries of all regions are kept perfectly insulated.

In the present study, various numerical simulations are being performed to analyze and compare thermoelectric performance of different configurations of PV/PCM system (Figure 5.1). Different cases are formed and analyzed on the basis of different lower thickness (L_1/L), extension ratio (H_e/H_{pv}) and right wall profile. For a particular lower thickness ratio (L_1/L), and right wall profile, the upper thickness ratio (L_2/L), and bifurcation mass ratio (m_{upper}/m_{lower}) changes with change in extension ratio(H_e/H_{pv}) which are indicators of compactness of system and PCM distribution in non-rectangular PCM enclosure respectively. All design specification on basis of these variables for all PV /PCM configurations with non-rectangular PCM enclosure are discussed in Table 5.1.

In this study design specification such as lower thickness ratio, extension ratio and profile of right wall is optimized in such a way that PV/PCM system obtains maximum thermo-electric performance. The incident solar radiation (I_{solar}), ambient temperature (T_a), and wind speed

Table 5.1: Design specifications for all PV /PCM configurations with non-rectangular PCM enclosure.

Type	**Lower thickness ratio**(L_1/L)								
	0.1			0.3			0.5		
	$\frac{H_e}{H_{pv}}$	$\frac{L_2}{L}$	$\frac{m_{upper}}{m_{lower}}$	$\frac{H_e}{H_{pv}}$	$\frac{L_2}{L}$	$\frac{m_{upper}}{m_{lower}}$	$\frac{H_e}{H_{pv}}$	$\frac{L_2}{L}$	$\frac{m_{upper}}{m_{lower}}$
	0	1.9	2.63	0	1.7	2.07	0	1.5	1.67
	0.1	1.72	3.27	0.1	1.52	2.47	0.1	1.32	1.92
B	0.2	1.57	3.93	0.2	1.37	2.83	0.2	1.17	2.13
	0.3	1.44	4.6	0.3	1.24	3.16	0.3	1.04	2.31
	0.4	1.33	5.26	0.4	1.13	3.46	0.4	0.93	2.47
	0	2.8	5.15	0	2.4	3.21	0	2	2.2
	0.1	2.53	6.49	0.1	2.13	3.7	0.1	1.73	2.42
C	0.2	2.3	7.8	0.2	1.9	4.09	0.2	1.5	2.59
	0.3	2.11	9.05	0.3	1.71	4.41	0.3	1.31	2.7
	0.4	1.94	10.21	0.4	1.54	4.67	0.4	1.14	2.79
	0	3.7	8.61	0	3.1	4.16	0	2.5	2.55
	0.1	3.34	10.36	0.1	2.74	4.6	0.1	2.14	2.71
D	0.2	3.03	12.07	0.2	2.43	4.91	0.2	1.83	2.82
	0.3	2.78	13.48	0.3	2.18	5.12	0.3	1.58	2.88
	0.4	2.56	14.63	0.4	1.96	5.27	0.4	1.36	2.92

(v_w) are taken 800 W/m^2, 20°C, and 2.4 m/s respectively.

5.2.3 Numerical solution

The conservation equations and other governing equation used for current investigations are shown by Eqs. 2.7-2.14. To discretize and solve conservation equations and other governing equations, the same assumptions and solution methodology as in section 2.2.2 (solution method) of chapter 2 are utilised. The current model of PV/PCM is also analysed for grid independence test that is better described in section 2.2.3 of chapter 2. Figure 2.2 depicts that a minimal deviation in results are reported beyond optimum number of grids and optimum value of time step.In PV/PCM system, the glass and PV cell region is governed by simple physics (conductive heat transfer only), while PCM region by rather complex physics (both conductive and natural convection dominated heat transfer, and phase change). At the same time, melting behavior of PCM governs the working of PV/PCM system, hence to validate numerical model emphasis must be given on natural convection driven melting of PCM region. Experimental work by Kamkari et al., [37] on natural convection driven melting within a rectangular enclosure is chosen and reproduced for numerical validation (see Figures 2.3 and 2.4). The comprehensive examination of experimental validation of the computational model, as well as error and limitations, is adequately described in section 2.2.4 of Chapter 2. It can be observed that the path of numerical curve and the experimental measurements are similar and exhibit negligible vari-

ance. Hence numerical model is presumed to capture the physics involved in the experimental setup.

5.3 Results and discussions

5.3.1 Solid-liquid interface patterns

Melting front morphology plays an important role in the performance enhancement of PV/PCM systems and develop a better understanding of heat transfer mechanism with in PCM enclosure. Figure 5.2(a), depicts the transient melting history of PCM inside a rectangular enclosure of type – A configuration of PV/PCM system. The incident radiation is absorbed by PV cell and channelized to PCM region through PV-PCM interface by means of conductive heat transfer. Initially the mode of heat transfer in solid PCM is also conductive and it raises the temperature of PCM to phase transition temperature which initiates the melting adjacent to PV-PCM interface. The melting front propagate parallel to PV-PCM interface until conductive heat transfer dominates in PCM enclosure and this regime of melting is termed as conduction regime of melting (up to 15 minutes approx. from incidence of radiation). The conduction regime ends with development of buoyant forces due to gravity in top region of enclosure while conduction still dominates the bottom region of enclosure, hence this regime is termed as mixed (conduction as well as convection) regime. The melting front doesn't remain parallel to PV-PCM interface anymore as erosion of solid-liquid interface takes place in top region and this erosion is clearly visible at 30 minutes of Figure 5.2(a). With progression of time, viscous forces (due to conduction) is completely dominated by buoyant forces (due to convection) in whole melted PCM region that gave rise to quasi-steady convection regime of melting. The solid-liquid interface become completely unsymmetrical to PV-PCM interface as melting rate is enhanced due to convection driven melting. This regime ends as solid-liquid interface reaches the right wall of the enclosure (after 56 minutes of incidence of radiation) which will give rise to solid-shrinking regime. The solid PCM shrinks along the right wall in this regime and melting decelerates due to thermal stratification. The solid-shrinking regime is depicted in 60 minutes, 90 minutes, and 120 minutes for rectangular enclosure of Figure 5.2(a).

The rectangular PCM enclosure of type – A configuration of PV/PCM system exhibit very short span of quasi-steady convection regime, hence thermo-electric performance of PV/PCM system gets degraded. It is clear that convection driven melting is dominated in top region of enclosure, therefore PCM enclosure must be designed according to melting front morphology and non-rectangular PCM enclosure is introduced in type – B, C, and D configurations of PV/PCM systems. While designing non-rectangular enclosure, many variables have come into consideration such as lower thickness ratio (L_1/L), upper thickness ratio (L_2/L), profile of right wall (linear, parabolic and cubic) and bifurcation mass ratio (m_{upper}/m_{lower}). Lower thickness ratio

is an indication of amount of PCM available for lower portion of PV panel and decides upper thickness ratio and bifurcation mass ratio as volume of PCM is constant (same of rectangular enclosure). The profile of right wall decides the type of configuration such as type – B for linear, type – C for parabolic, and type – D for cubic profile of right wall. The upper thickness ratio is an indication of compactness of enclosure and bifurcation mass ratio is an indication of PCM distribution with in enclosure. All these variables needs to be optimized so that thermo-electric performance get maximized.

Figure 5.2(b) depicts the transient melting history for type – B configuration (for lower thickness ratio of 0.3) respectively. The conduction and mixed regime of melting is same as that of type – A configuration but quasi-steady convection regime got extended due to availability of more PCM in top region of enclosure hence thermo-electric performance of PV/PCM system. The quasi-steady convection regime extends up to 84 minutes for type – B configuration. However, the quasi-convection regime extends to 116 minutes for type – C, and it doesn't end during 120 minutes of process for type – D configuration. Type – C and type – D configuration exhibit a significant improvement but high upper thickness ratio (2.4 for type – C and 3.1 for type – D) and bifurcation mass ratio (3.21 for type – C and 4.16 for type – D) allows PCM in lower region to reach the right wall which will degrade its performance a bit and compactness of system is also lost (see Table 5.1). Further, type – B configuration needs further improvement regarding enlargement of quasi-steady convection regime. Hence, design improvement is further desired and extended non-rectangular enclosure is advised for a compact and high performance PV/PCM system.

Melting front morphology of extended PCM enclosure is little different than the aligned one. The melting is initially governed by conductive and very similar to aligned PCM enclosure (up to 15 minutes approx.) while the regimes beyond conduction regime are a bit different. In mixed regime of melting, the melting front tries to penetrate in the extended part of enclosure as a result of convection generated near top part of PV-PCM interface. The penetration of melting front in extended part is clearly visible at 30 minutes of Figure 5.2(c – e), and similar for all studied extension ratio (0.1 – 0.4) for all type of non-rectangular configurations (B, C, and D). Now, melting front are free to move in horizontal direction (towards right wall of enclosure) and vertical direction (towards top wall of enclosure). Hence, melting front propagates like a swallowing balloon in horizontal and vertical direction that is clearly visible at 60 minutes in Figure 5.2(c – e), and for all type of non-rectangular configurations (B, C, and D) and all extension ratio (0.1 – 0.4). The mixed regime of melting ends with development of convection current in whole liquid region but the span of quasi-convection regime is quite complex for extended enclosure as convection driven melting is present even after melting front reaches either top wall or right wall of enclosure. However, end of quasi-convection regime is decided with end of convection driven melting either due to less availability of PCM in upper region or due to thermal stratification. The timing of melting front to reach top and right wall is shown in Table 5.2.

Table 5.2: Timing of melting front reaching right and top wall for all non-rectangular configurations. Note 120* indicates that melting front does not reach the respective wall in 120 minutes of process.

$\frac{L_1}{L}$	$\frac{H_e}{H_{pv}}$	Time (Melting Front reaches top wall) in minutes			Time (Melting Front reaches right wall) in minutes								
					At $0.5H_{pv}$			At $0.75H_{pv}$			At or above H_{pv}		
	Type	**B**	**C**	**D**	**B**	**C**	**D**	**B**	**C**	**D**	**B**	**C**	**D**
0.1	0.1	44	46	52	120*	105	72	120*	120*	120*	107	120*	120*
	0.2	70	78	86	120*	92	50	120*	120*	112	120*	120*	120*
	0.3	103	110	120*	120*	74	35	120*	108	84	120*	120*	120*
	0.4	120*	120*	120*	110	54	28	113	82	65	114	105	91
0.3	0.1	44	46	52	120*	120*	97	120*	120*	120*	99	120*	120*
	0.2	70	78	86	120*	116	91	120*	120*	113	112	120*	120*
	0.3	103	120	114	120*	105	81	120*	120	97	120*	120*	120
	0.4	120*	120*	120*	116	91	70	107	97	80	102	98	89
0.5	0.1	44	44	47	120*	120*	120*	111	120*	120*	90	107	120*
	0.2	70	71	85	120*	120*	120*	116	120*	120*	103	119	120*
	0.3	103	114	118	120*	120*	114	115	112	106	105	115	100
	0.4	120*	120*	120*	114	108	100	99	97	92	89	91	89

Melting front reaches the top wall earlier than right wall at low extension ratio and it reaches right wall earlier than top wall at high extension ratio. This is due to fact that upper thickness ratio decreases and bifurcation mass ratio increases with extension ratio for a given lower thickness ratio (see Table 5.1). The right wall is at unequal distance from PV panel along the height of PV panel due to non- rectangular shape of enclosure and profile of right wall. Therefore, timing of melting front approaching to right wall is studied at three different location to better understand the melting front morphology. It can be concluded from the Table 5.2 and Figure 5.2 that melting front morphology is greatly affected by profile of right wall, lower thickness ratio and extension ratio as these variable affects the mass distribution with in the enclosure and compactness of enclosure. Thus, shape of PCM enclosure is optimized in way that duration of convection driven melting increases with decrease in solid shrinking regime.

The PCM enclosures with lower thickness ratio of 0.1 possess very low amount of PCM in lower half of enclosure for all type of configuration. Hence, these enclosures are not recommended as strength of convection current is not enough due to thermal stratification in lower region even if melting front in upper region doesn't touch the wall. This exact problem arises for high extension ratios (0.3 and 0.4) in type – C and type – D configuration even lower thickness ratio possess higher value of 0.3 and 0.5. Therefore, optimization of shape of enclosure is done

for better melting front morphology so that maximum span of convection driven melting can lead to better thermo-electric performance. The optimization is achieved at moderate values of extension ratio (0.3 for type – B configuration, and 0.2 for type – C and type – D configuration) at moderate lower thickness ratio (0.3 for type – B configuration, and 0.5 for type – C and type – D configuration). However, type – B configuration can be recommended for the sake of simplicity of design, ease of manufacturing and compactness. It can now be established that modified designs are more suitable for PV/PCM systems to work more efficiently as these designs conforms to the gravity driven convective currents.

5.3.2 Temperature distributions

Melting front morphology also decides the temperature distribution with in enclosure which affects the temperature of PV panel and thus electric performance of PV/PCM system. Therefore, it is necessary to understand the transient variation of temperature comparative to melting front propagation. Transient history of temperature contours along with solid fraction contours for type – B configuration ($L_1/L = 0.3$,and $H_e/H_{pv} = 0.3$) of PV/PCM system are shown in Figure 5.3. Solid fraction contours are attached like mirror image to temperature contour to get better understanding of the process. Temperature is an indication of absorption of sensible heat by PCM as latent heat is absorbed at constant phase transition temperature. Therefore, liquid PCM will always absorb more sensible heat compared to solid PCM. Figure 5.3(a) depicts the beginning of convection where convection current is fully developed with in liquid region and melting front starts penetrating in extended part of enclosure. Temperature distribution contour follow the same trend and a temperature gradient of 3.76°C is observed along PV-PCM interface with lower temperature of 29.55 °C at the bottom of the interface. However, sensible heat penetration in extended part of enclosure is low (temperature is 20.68°C in extended solid region) as heat is diffused in extended region from the penetrated melting front only. Thus melting front is the only heat carrier to extended part.

With progression of time, melting front develops fully in extended region and expands like a swallowing balloon inside PCM enclosure that allows spread of incoming heat with in enclosure effectively. A flame like plume is observed in extended part of the enclosure in Figure 5.3(b) and (c) at 60 minutes and 90 minutes of the process. The temperature gradient along the PV-PCM interface doesn't change that much with time (3.89°C at 120 minutes) as heat is carried away from it by accelerated convection current. However, the temperature in top extended part approaches to 31.55°C as melting front touches the right wall at 103 minutes of process. It is concluded that thermal stratification can be maintained at low level if convective melting is maintained for longer duration then level. The demonstrated configuration of extended non-rectangular enclosure in Figure 5.3 exhibit the longer convective melting thus lower thermal stratification and lower PV panel temperature.

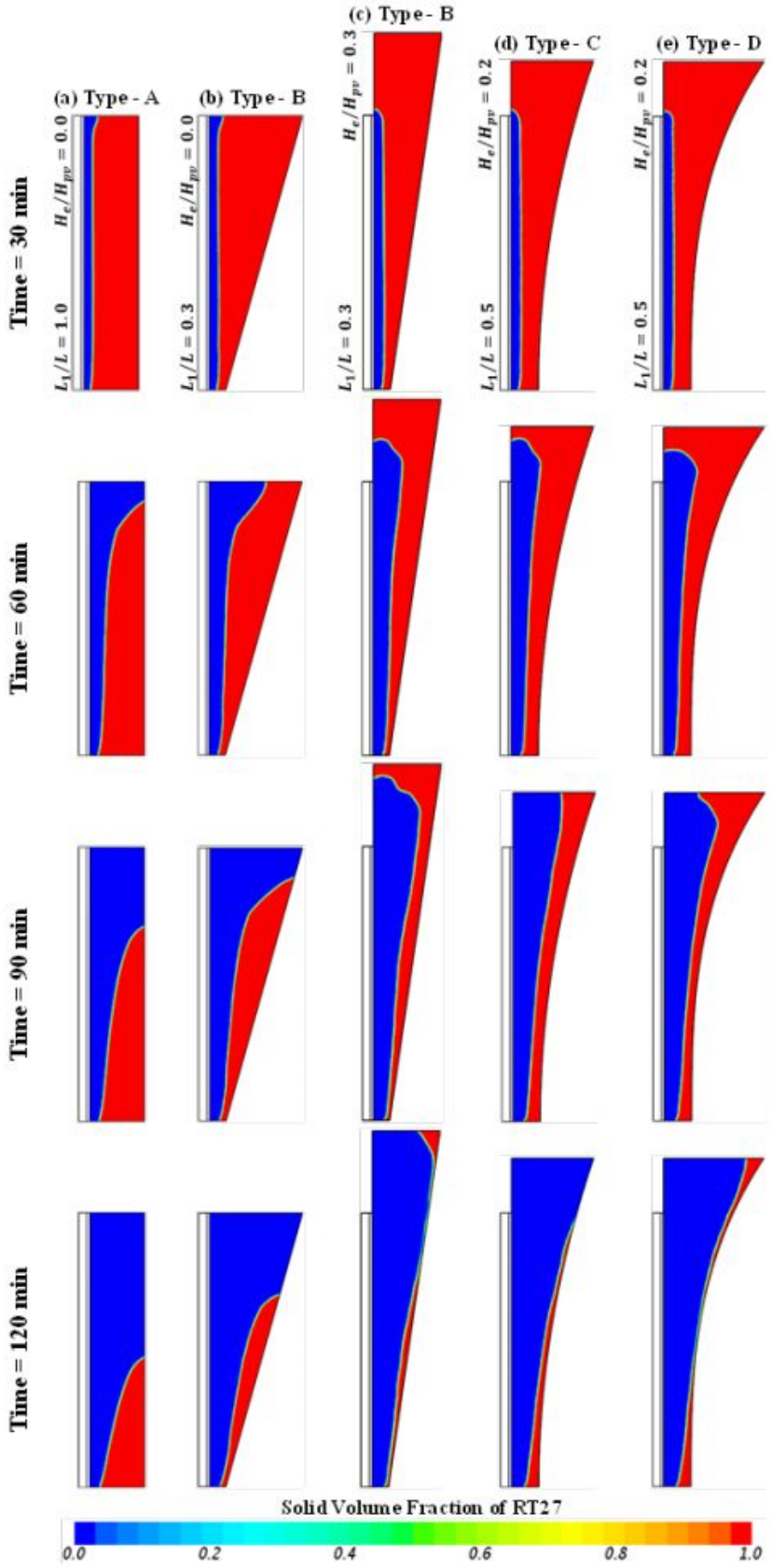

Figure 5.2: Transient history of solid-liquid interface patterns for different configurations of PV/PCM system.

Further, comparison of temperature distribution among different configuration of PV/PCM system at 120 minutes is demonstrated in Figure 5.4. The convection regime in type – A configuration (rectangular PCM enclosure) ends very soon (56 minutes only) which causes a high level of thermal stratification with in PCM enclosure due to more absorbed sensible heat by liquid PCM. The temperature gradient along PV-PCM interface approaches a value of 16.92°C which rises the PV panel temperature enormously and degrades its electric power producing ability. Modification of design of PCM enclosure to non-rectangular (type – B, C and D) reduces this level of thermal stratification due to extended convection regime. In type – B configuration, the temperature gradient along PV-PCM interface decreases to 9.86°C with temperature in bottom region approaches to 29.6°C. Extended enclosure further enhances the uniformity of temperature distribution with in PCM enclosure which results in better PV panel performance. The temperature gradient along PV-PCM interface first decreases with extension ratio (decreases up to extension ratio of 0.3) and then starts increasing at a given lower thickness ratio for type – B configuration. Type – B configuration exhibits lowest value of temperature gradient of 3.89°C with bottom side temperature of 29.58°C for extension ratio of 0.3. Further type – C and D configuration of PV/PCM system exhibits similar temperature distribution to type – B configuration at higher value of lower thickness ratio (0.5) and lower value of extension ratio (0.2). However, these configuration exhibits higher temperature distribution in the bottom region of enclosure is higher due availability of low amount of PCM at smaller values of lower thickness ratio (0.1 and 0.3). Thus, type – C and type – D configuration always exhibits higher vlaues of temperature than type – B configuration at smaller values of lower thickness ratio.

The type – C and D configuration of PV/PCM system ($H_e/H_{pv} = 0.2, L_1/L = 0.5$) optimized the distribution of PCM inside the enclosure according to convective melting morphology which allows uniform distribution of heat inside the enclosure. The uniform melting leads to uniform temperature distribution, however; type – B configuration at lower thickness ratio of 0.3 and extension ratio of 0.3 maintains a better temperature uniformity and lower PV cell temperature than any other configuration due to better characterization of melting. In addition to that type – B configuration is more compact (upper thickness ratio of 1.24) and simpler geometry to manufacture, hence it is most preferred configuration of PV/PCM system.

5.3.3 Heat transfer characteristics

5.3.3.1 Melting process

Melting of PCM in any enclosure is categorized into four different regimes namely conduction, mixed, quasi-convection, and solid shrinking regimes based on type of heat transfer. To get a better understanding of melting process transient variation of liquid fraction is plotted in Figure 5.5 for type – B enclosure (at lower thickness ratio $L_1/L = 0.3$ for all extension ratios) and compared to type – A enclosure. Liquid fraction is an indicator of part of PCM turns into liq-

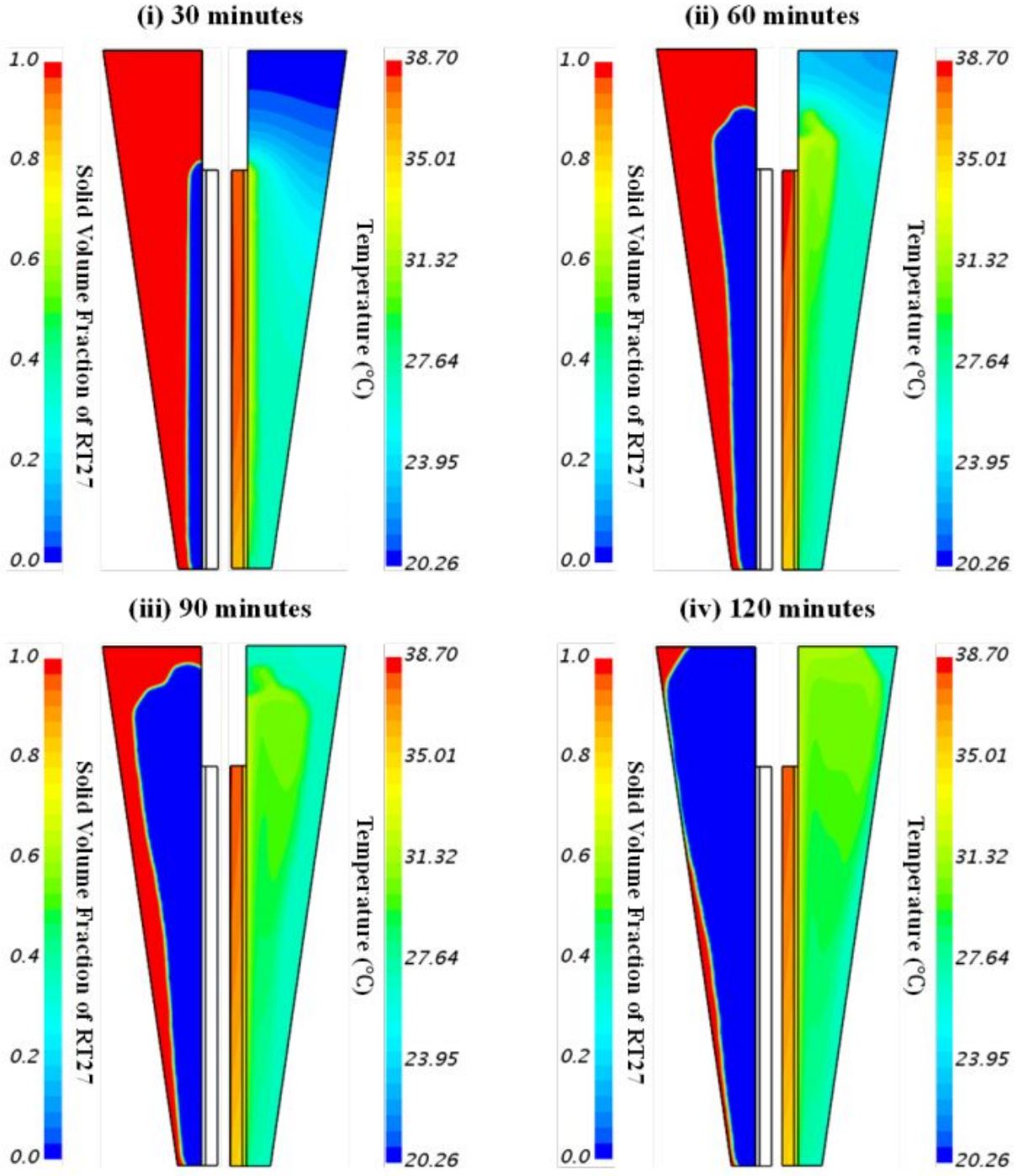

Figure 5.3: Transient history comparison of melting front contours with temperature distribution contours for type – B configuration of PV/PCM system at lower thickness ratio ($L_1/L = 0.3$) and extension ratio ($H_e/H_{pv} = 0.3$).

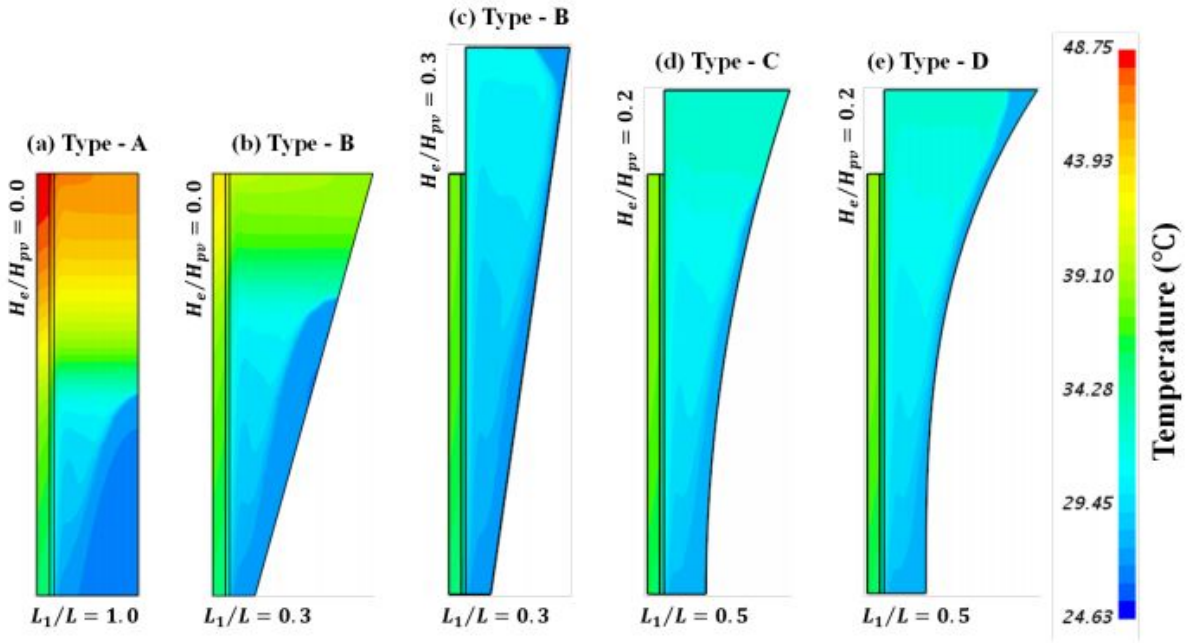

Figure 5.4: Temperature distribution at 120 minutes for different configurations of PV/PCM systems at lower thickness ratio .

uid by absorbing heat. For first three regimes of melting, liquid fraction varies linearly with time but melting rate in mixed and convection regime are higher due to accelerated convection current. However, convection current is decelerated in solid shrinking regime due to growing thermal stratification which cause melting to slow down. The transient variation of liquid fraction changes to curvilinear trend in solid shrinking regime of melting and slope of this curve decreases with progression of time.

In type – A configuration of PV/PCM system, solid shrinking regime starts at 56 minutes of the process due to which melting slows down and system exhibits 75.17% melting during 120 minutes (duration of incident radiation). The longer duration of solid shrinking regime allows liquid PCM exhibit growing thermal stratification and thus degrades electric performance of the system. In type – B configuration, the start of solid shrinking regime is delayed to 84 minutes and system exhibits 83.07% of melting which is 10.51% higher than type – A configuration of system. However, the duration of convection dominated melting can be increased to 120 minutes (see Table 5.2) by using extended type of non-rectangular enclosure. Type – B configuration at extension ratio of 0.3 and lower thickness ratio of 0.3 exhibit 90.58% of melting during 120 minutes which is 20.5% higher than type – A configuration and 9.04% higher than simple type – B configuration of same lower thickness ratio. Type – B configuration exhibit degradation in melting characteristics beyond extension ratio of 0.3 for lower thickness ratio of 0.3. Hence, it can be concluded that duration of convection dominated melting increases in extended enclosures for an optimized extended height.

The effect of extension ratio on melting of PCM for all type of enclosures at all studied lower

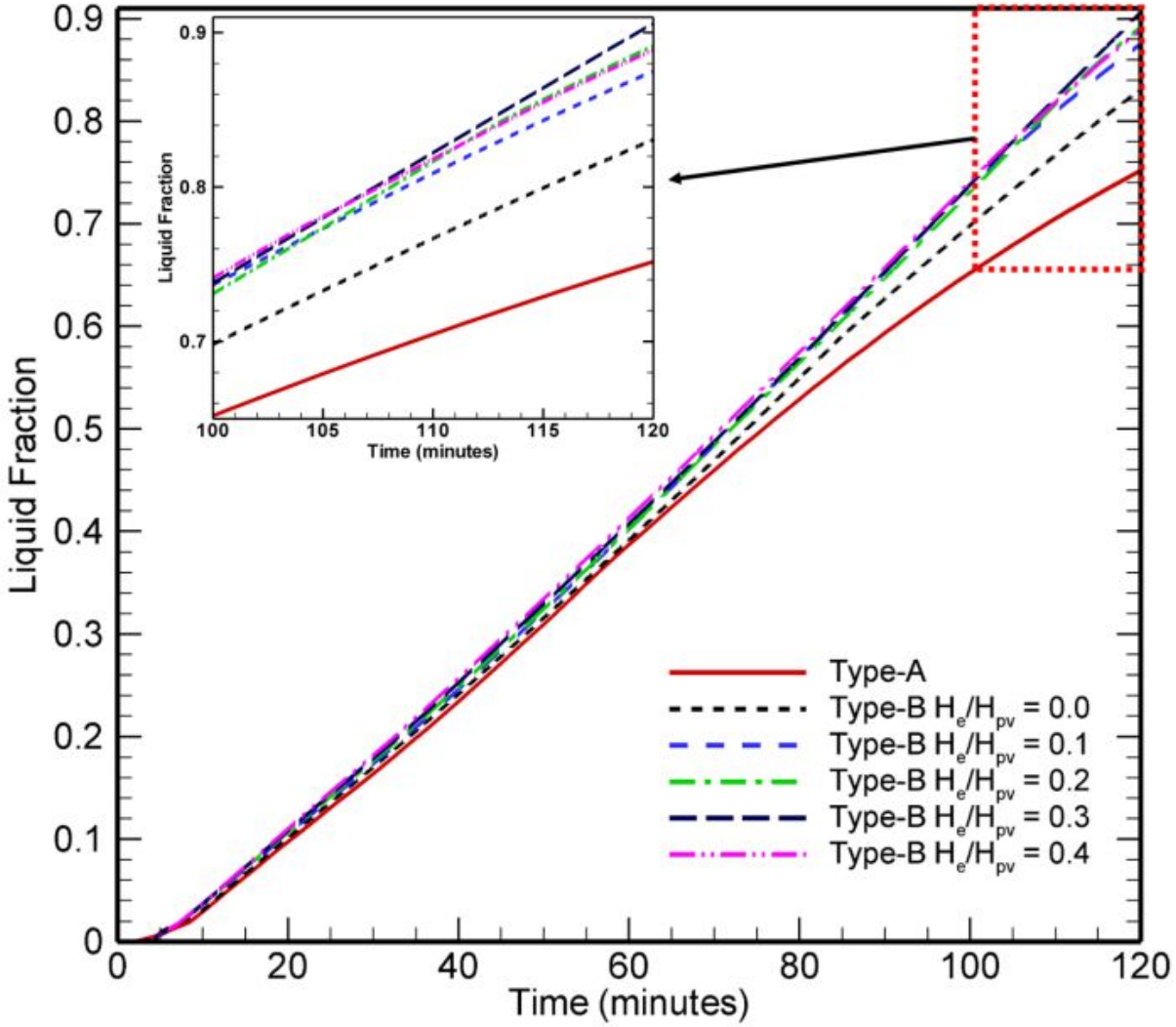

Figure 5.5: Transient variation of liquid fraction for type – B configuration of PV/PCM system at lower thickness ratio ($L_l/L = 0.3$). Expanded view of selected part of curve is shown in inset.

thickness ratio is mentioned in Figure 5.6 where the value of liquid fraction at 120 minutes is plotted at all studied extension ratio for all type of configurations. The optimum value of extension ratio is different for different lower thickness ratio for type – B configuration of non-rectangular enclosure. At lower thickness ratio of 0.1, type – B configuration exhibit a maximum melting of 89.33% at an extension ratio of 0.2, while for lower thickness ratios of 0.3 and 0.5, the optimum extension ratio is 0.3 with maximum melting of 90.58% and 88.90% during 120 minutes of process. Type – C configuration exhibit degradation in melting on increasing extension ratio for lower thickness ratio of 0.1, while enhancement of melting is observed in extended enclosures for higher values of lower thickness ratio till optimum extension ratios. For type – C configuration, optimum extension ratio is 0.1 for lower thickness ratio of 0.3 where 89.69% melting is observed and beyond this extension ratio melting is degraded. Whereas for lower

thickness ratio of 0.5, type – C configuration exhibits a melting of 89.79% at an optimum extension ratio of 0.2 during 120 minutes. Type – D configuration allows more PCM in upper half of enclosure, hence due to availability of lesser PCM in lower part of enclosure, this configuration exhibit degradation in melting on increasing the extension ratio for lower thickness ratio of 0.1 and 0.3 respectively. However, increment in melting is observed up to an optimum extension ratio of 0.2 for lower thickness ratio of 0.5, where 89.7% melting is observed and beyond it melting degrades with increase in extension ratio. It can be concluded that different configurations exhibit maximum melting performance at different extension ratios for different lower thickness ratio. Optimum extension ratio ensures efficient distribution of PCM inside enclosure so that maximum PCM is available for convection dominated melting for maximum duration for a given lower thickness ratio and right wall profile of enclosure.

All type configurations at their optimum extension ratios and lower thickness ratios exhibit approximately similar melting performance. However, type – B configuration at lower thickness ratio of 0.3 and extension ratio of 0.3 exhibits maximum melting of 90.58% and this configuration is also more compact ($L_2/L = 1.36$) among all better performing configurations, hence it is recommended for better thermos-electric performance of PV/PCM systems.

5.3.3.2 Nusselt number

Nusselt number is a dimensionless number which is an indicator for measuring the strength of heat transfer to the fluid from any surface or boundary. Transient variation of Nusselt number at PV-PCM interface for type – B configuration of PV/PCM system at lower thickness ratio of 0.3 and at all extension ratios is shown in Figure 5.7 and compared with type – A configuration. Nusselt number (Nu) along PV-PCM interface at any instant of time(t) can be given by Eq. 2.15.

Initially during conduction regime, the value of Nusselt number is very high despite of absence of convective melting due to very small thickness of melted PCM. Nusselt number exhibit decrement with increase in melting with increase in thickness of liquid PCM in conduction regime of melting. The conduction regime prevails from beginning of melting (at approx. 5 minutes) to the time when convection current develops in top region of enclosure (at approx. 15 minutes) which give rise to mixed regime of melting. Nusselt number still decreases till buoyant forces overcomes the viscous forces (at approx. 30 minutes). After this, quasi-steady convection regime starts where buoyant forces are developed in full melted region of PCM. Nusselt number is approximately constant in quasi-steady convection regime and starts to decrease linearly in solid-shrinking mode of melting due to retardation of convection current.

In type – A configuration of PV/PCM system, quasi-steady convection regime ends at 56 minutes of process and Nusselt number starts to decrease and approaches to 28.04 at 120 minutes. Type – B configuration at lower thickness ratio of 0.3 exhibits extended quasi-convection regime of 84 minutes which enhances the value of Nusselt number to 36.61 at 120 minutes of

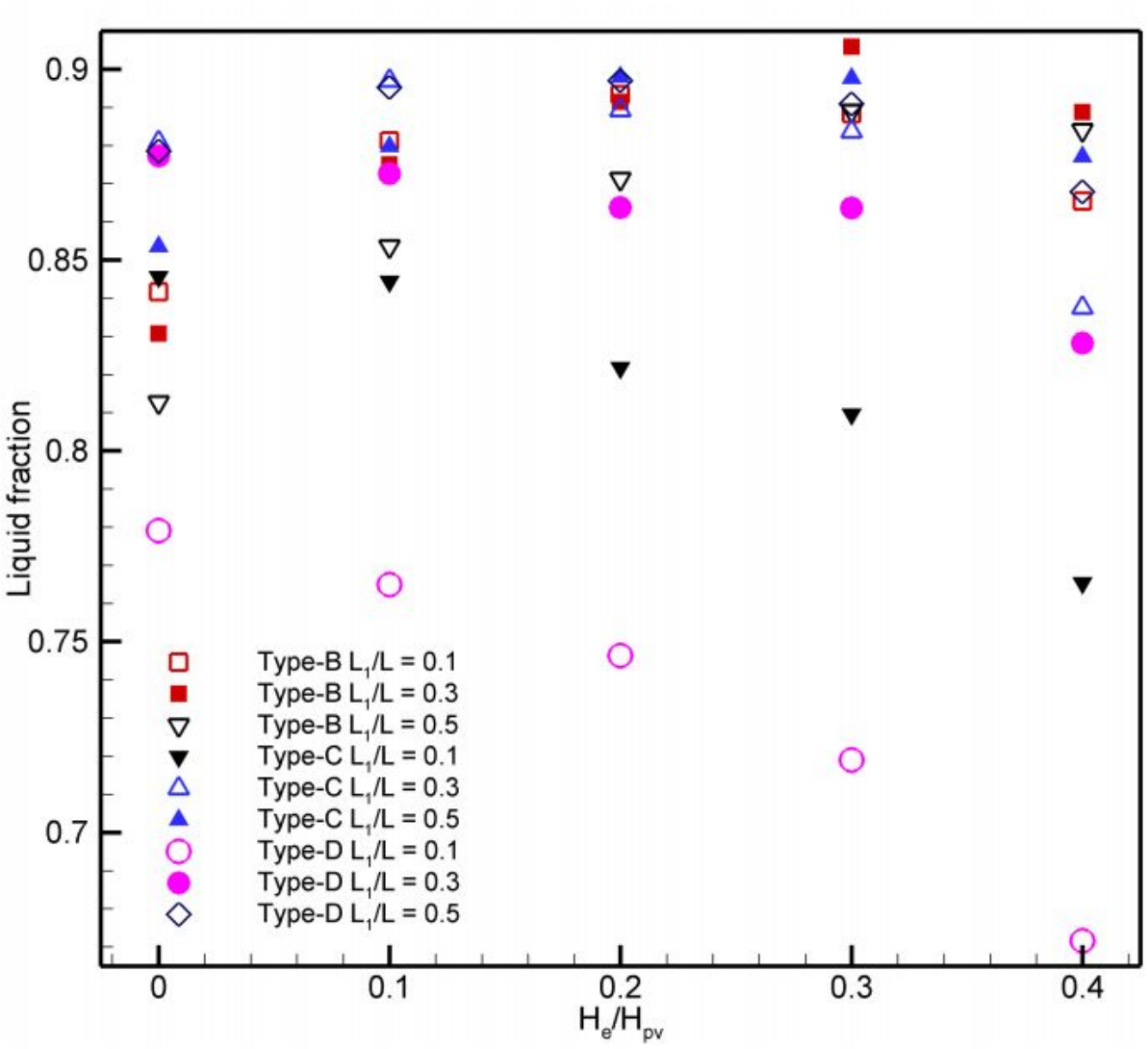

Figure 5.6: Fraction of liquid melted after 120 minutes of process for all configurations of PV/PCM system with non-rectangular PCM enclosure.

process which is 30.56% higher than type – A configuration of PV/PCM system. Further, duration of convection dominated melting regime increases in extended enclosures of type – B configuration. Nusselt number first increases with extension height up to an optimum extension ratio and then decreases for type – B configuration. The optimum extension ratio for type – B configuration at lower thickness ratio of 0.3 is found to be 0.3 at which Nusselt number attains maximum value of 46.79 at 120 minutes. Nusselt number for extended type – B configuration ($H_e/H_{pv} = 0.3, L_1/L = 0.3$) exhibits 66.87% improvement compared to type – A configuration and 27.81% compared to aligned type – B configuration. This improvement in heat extracting ability of the system is just due to efficient PCM distribution with in enclosure so that maximum PCM can be available for convection dominated melting for maximum duration.

Further, the effect of extension ratio on Nusselt number for different configuration of non-

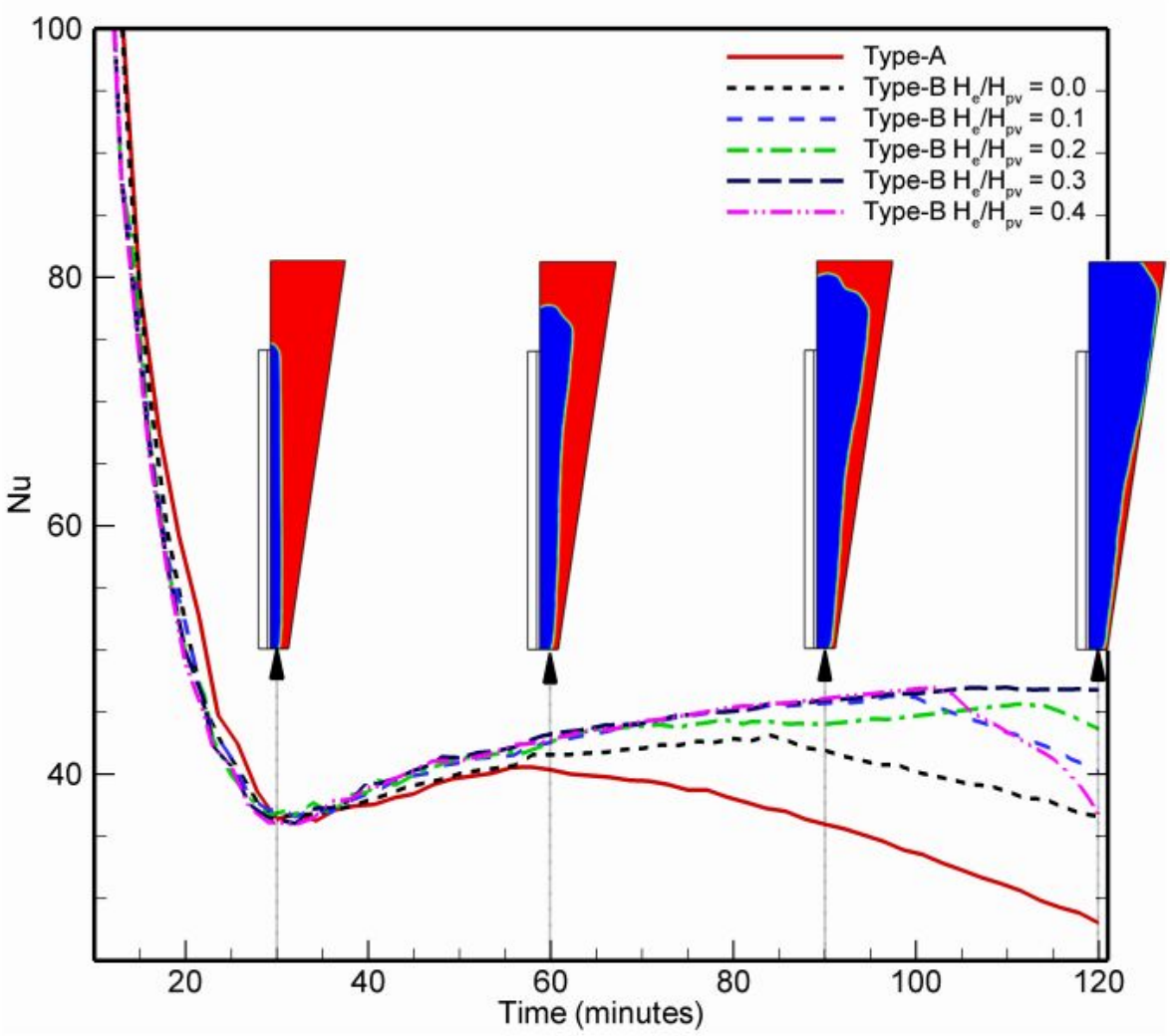

Figure 5.7: Variation of Nusselt number with time for type – B configuration of PV/PCM system at lower thickness ratio ($L_1/L = 0.3$). Transient history of melting front contours for same configuration at extension ratio ($H_e/H_{pv} = 0.3$) is shown in inset.

rectangular enclosure at different lower thickness ratio is shown in Figure 5.8. The optimum extension ratio exhibit same trend for Nusselt number as it shows for liquid fraction for all type of configuration. The most efficient design of PCM enclosure for type – C configuration is at lower thickness ratio of 0.5 and extension ratio of 0.2 which exhibit the value of Nusselt number of 45.1 that is 60.84% more efficient than type – A configuration and 20.65% more efficient than its own aligned counterpart of type – C configuration. For type – D configuration, the optimum extension ratio and lower thickness ratio are 0.2 and 0.5 respectively. Nusselt number exhibits 45.64 at 120 minutes for most efficient type – D configuration which is 62.77% more efficient than type – A configuration and 9.74% more efficient than its own aligned counterpart of type – D configuration. However, the most efficient configuration of PV/PCM system is extended type – B configuration ($H_e/H_{pv} = 0.3, L_1/L = 0.3$) and it also exhibit more compactness ($L_2/L =$

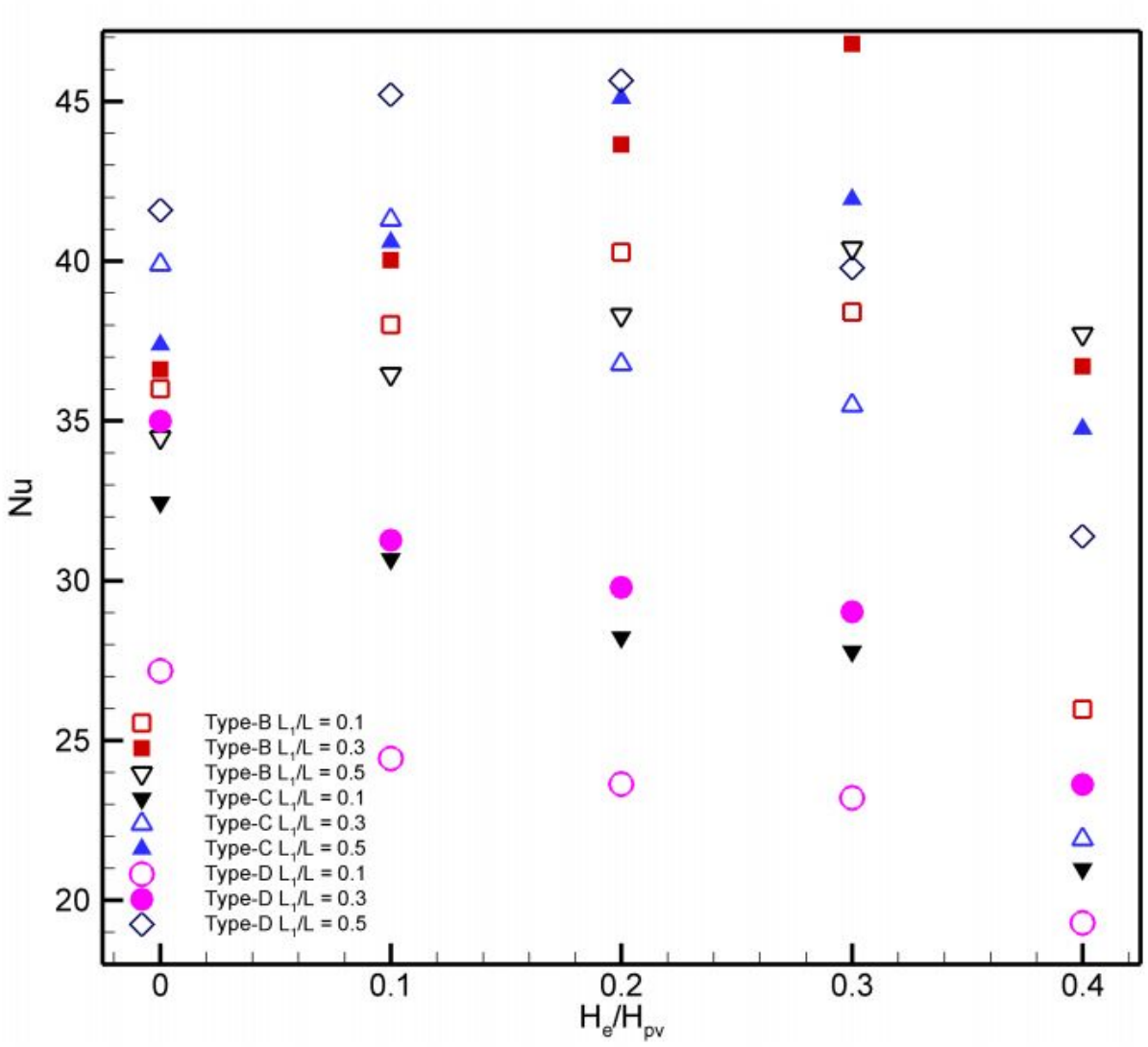

Figure 5.8: Comparison of Nusselt number at 120 minutes of process among all configuration of PV/PCM system with non-rectangular PCM enclosure.

1.36) compared to most efficient type – C configuration ($L_2/L = 1.36$) and type – D configuration ($L_2/L = 1.36$) respectively. Hence it is most recommended and most efficient configuration of PV/PCM system with improved thermo-electric performance.

5.3.3.3 Thermal energy storage performance

The performance of PV/PCM system is also determined by its ability to store heat that can be stored as latent heat as well as sensible heat. Energy storage density *(ESD)* is one of the parameter that can indicate the heat storing ability of PCM enclosure. *ESD* is the maximum possible derivable energy from the system and can be defined by Eq. 2.16.:

Where, first term '$\rho c_p \Delta T$' is sensible energy storage density *(SESD)* which arises due to temperature gradient 'ΔT' that can be defined as $\Delta T = T_{PCM} - T_{initial}$ with T_{PCM} as local PCM

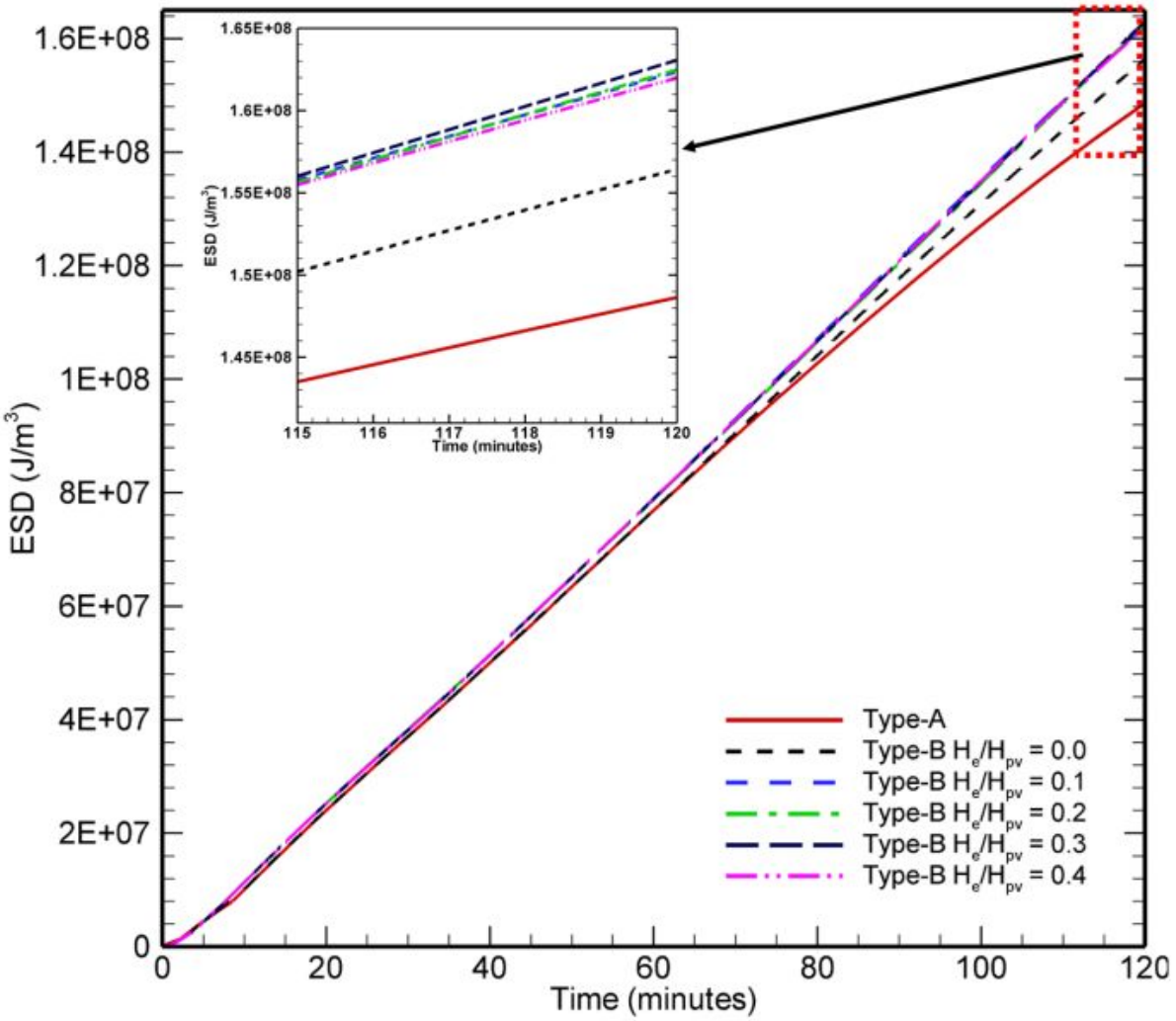

Figure 5.9: Transient variation of energy storage density *(ESD)* for type – B configuration of PV/PCM system at lower thickness ratio ($L_V/L = 0.3$). Expanded view of selected part of curve is shown in inset.

temperature and $T_{initial}$ is the initial temperature. The second term '$\rho f_l L_{sf}$' is latent energy storage density *(LESD)* which is required to melt f_l fraction of PCM by absorbing L_{sf} amount of latent heat.

Figure 5.9 exhibits the transient variation of *ESD* for type – B configuration ($L_V/L = 0.3$) for all extension ratios and compared to type – A configuration of PV/PCM system. *ESD* follows the trend similar to liquid fraction as *LESD* major contributing potion compared to *SESD*. Hence, type – A configuration exhibits decreasing slope curvilinear nature after the end of quasiconvection regime. The aligned configuration of type – B configuration ($H_e/H_{pv} = 0.0, L_V/L = 0.3$) exhibit increment in quasi-convection regime, therefore it exhibit an improvement of 5.24% in *ESD* compared to type – A configuration. *ESD* first increases with extension ratio and then decreases after reaching an optimum value of extension ratio for type – B configuration. For lower

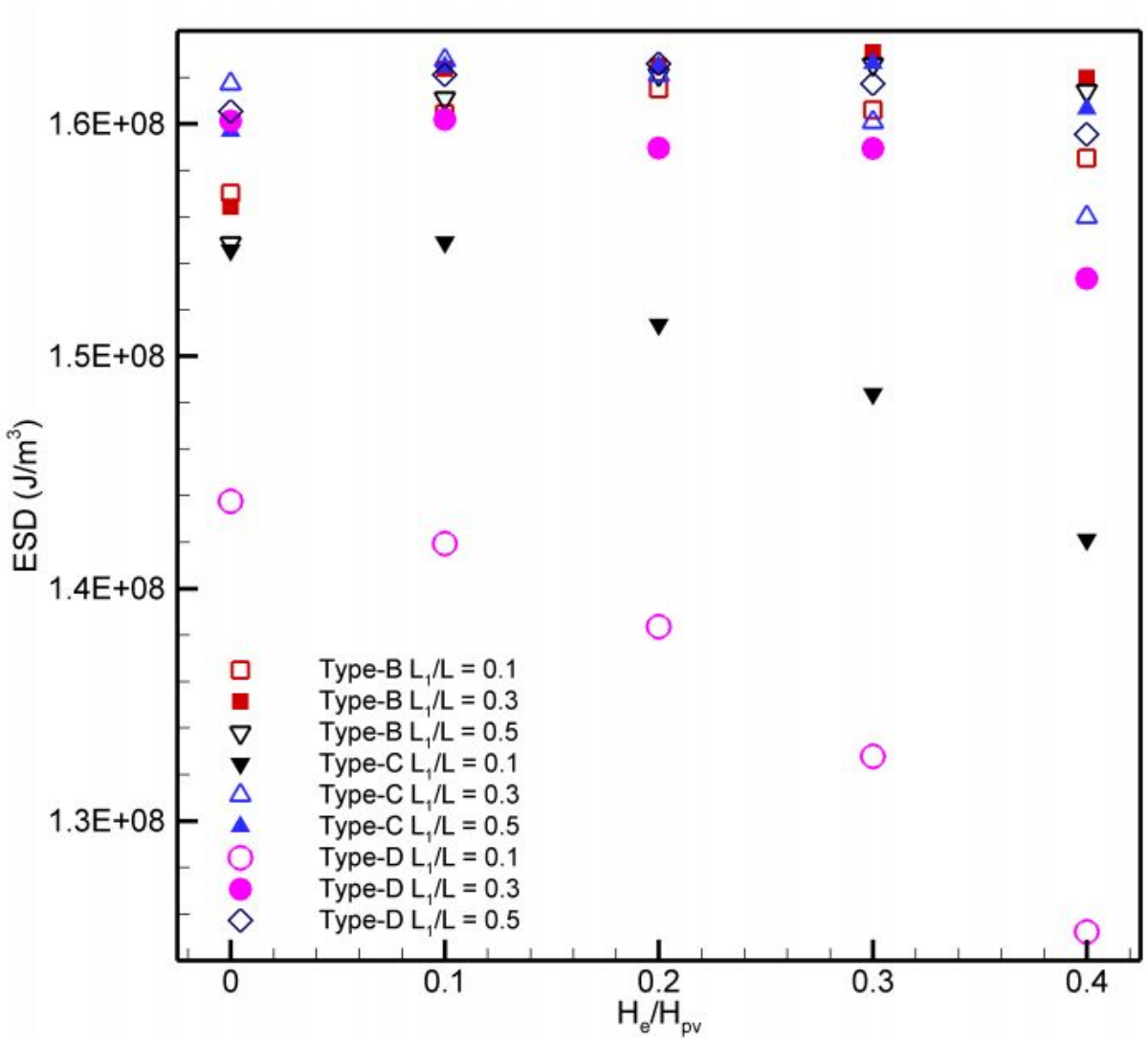

Figure 5.10: Comparison of *ESD* at 120 minutes of process among all configuration of PV/PCM system with non-rectangular PCM enclosure.

thickness ratio of 0.3, the optimum extension ratio is found to be 0.3 at which *ESD* exhibit an improvement of 9.71% compared to type – A configuration and 4.26 % compared to type – B configuration ($H_e/H_{pv} = 0.0, L_1/L = 0.3$). This improvement is due to enhanced duration of convection dominated melting due to efficient distribution of PCM with in the enclosure that allows linear variation of *ESD* with time for longer duration.

Further, the effect of extension ratio on *ESD* for all type of configuration of PV/PCM system is demonstrated in Figure 5.10. Since *ESD* is directly dependent on liquid fraction, hence similar dependency over extension ratio is observed at given right wall profile and lower thickness ratio. Type – C configuration exhibit continuous degradation in *ESD* with extension ratio for $L_1/L = 0.1$, however at $L_1/L = 0.3$ the optimum extension ratio is 0.1 at which an improvement of 9.48% compared to type – A configuration and 0.63% improvement compared to type

– C configuration ($H_e/H_{pv} = 0.0, L_1/L = 0.3$). At a lower thickness ratio of 0.5, the optimum extension ratio is 0.2 for type – C configuration which is 9.32% more efficient than type – A configuration and 1.76% more efficient than type – C configuration ($H_e/H_{pv} = 0.0, L_1/L = 0.5$). However, type – D configuration exhibit continuous degradation in *ESD* with extension ratio for both $L_1/L = 0.1$ & 0.3. While at $L_1/L = 0.5$ the optimum extension ratio is 0.2 at which an improvement of 9.39% compared to type – A configuration and 1.28% improvement compared to type – D configuration ($H_e/H_{pv} = 0.0, L_1/L = 0.5$). The optimum extension ratio is also different for different lower thickness ratio for type – B configuration, i.e, at $L_1/L = 0.1$ the optimum H_e/H_{pv} is 0.2 and at $L_1/L = 0.3$ & 0.5 the optimum extension ratio is 0.3. However, type – B configuration ($H_e/H_{pv} = 0.3, L_1/L = 0.3$) exhibits better heat storage performance than any other configuration and also it has better compactness than extended type – C and D configuration of PV/PCM system. Hence, this configuration is not only recommended for better electric performance but also for a better heat storage performance.

5.3.4 Performance characteristics

5.3.4.1 Effect of PV cell temperature on power conversion efficiency

The effect of PV cell temperature on its electric conversion performance is given by Eqn. 2.14 which states that electric conversion efficiency degrades from its reference value with rise in temperature of PV panel. Figure 5.11 depicts the transient variation of PV panel temperature and its effect on electric conversion efficiency for type – B configuration (for all extension ratio at lower thickness ratio of 0.3) of PV/PCM system comparatively to type – A configuration and no PCM configuration of the system. PV panel temperature rises to 56.78°C and its efficiency deteriorates to 10.84% for no pcm configuration of the system. In PV/PCM system, the temperature of PV panel is controlled by melting process of PCM enclosure. In type – A configuration of system, PV panel temperature rises to 32.12°C by the end of conduction regime and 34.86°C by the end of mixed regime of melting. In convection regime, convection current starts to accelerate and PV panel temperature starts to decrease till the end of quasi-convection regime (56 minutes). The melting process slows down in solid shrinking regime due to retardation of convection current that make temperature to increase to 39.28°C by the end of 120 minutes. Electric conversion efficiency is inversely dependent on PV panel temperature, hence PV panel efficiency approaches to 11.69% by the end of 120 minutes of process. This is an improvement of 7.84% in electric conversion efficiency as operating temperature of PV panel is decreased by 30.82% compared to conventional PV system. However, there is possibility of decreasing temperature of PV panel and increasing its electric performance by increasing the span of quasi-convection regime. In type – B configuration ($H_e/H_{pv} = 0.0, L_1/L = 0.3$) of PV/PCM system, the span of quasi-convection regime increase to 84 minutes which cause PV panel temperature to drop to 35.99°C and efficiency to rise to 11.86%. Further, the usage of extended non-rectangular

enclosure allows more PCM for convection dominated melting for longer duration. The performance of PV panel first increases up to optimum extension ratio due to decrease in PV cell temperature and after that it decreases.

Type – B configuration ($H_e/H_{pv} = 0.3, L_1/L = 0.3$) of PV/PCM system exhibit lowest PV panel temperature of 34.21°C at the end of 120 minutes. This is 39.74% lesser than no PCM configuration, 12.91% compared to type – A configuration, and 4.95% compared to Type – B configuration ($H_e/H_{pv} = 0.0, L_1/L = 0.3$) of PV/PCM system. As a consequence, PV cell efficiency approaches to 11.95% which is 96.37% closer to its reference value which is a significant improvement compared to conventional PV system (87.41 % of η_{ref}), type – A configuration of PV/PCM system (94.27 % of η_{ref}), and aligned type – B configuration of PV/PCM system (95.64 % of η_{ref}). Further, comparison of PV cell temperature and electric conversion efficiency for all configurations at different extension ratios and lower thickness ratios are given in Figure 5.12. Electric performance of PV panel is affected by PV panel temperature which is controlled by melting behavior of PCM, hence optimum extension ratio is same for these parameters that was for liquid fraction in all type of configurations. Type – C and D configurations of PV/PCM system exhibit maximum electric performance at $H_e/H_{pv} = 0.2$, and $L_1/L = 0.5$. Both configuration exhibit electric conversion efficiency of 11.94% with PV cell temperature of 34.36°C for type – C and 34.34°C for type – D configuration respectively. Type – B configuration ($H_e/H_{pv} = 0.3, L_1/L = 0.3$) exhibit marginally enhanced electric performance compared to Type – C configuration ($H_e/H_{pv} = 0.2, L_1/L = 0..5$), and Type – D configuration ($H_e/H_{pv} = 0.2, L_1/L = 0.5$). However, Type – B configuration ($H_e/(H_{pv} = 0.3, L_1/L = 0.3$) is recommended due to more compactness and simplified geometry.

5.3.4.2 Overall system performance

Overall performance of the system can be estimated by analyzing the ability of system to utilize incoming radiation. Total utilized radiation ($I_{utilized}$) is the part of incident radiation that is absorbed either in form of electric power or stored heat is by the system. Total utilized radiation is sum of electric power output and stored heat. At any instant of time, it can be given by Eq. 4.1.

The remaining part of incoming radiation that is lost to surrounding is termed as unutilized radiation ($I_{unutilized}$) and defined by Eq. 4.2.

Figure 5.13 depicts the comparison of transient variation of total utilized radiation among conventional PV system, type – A configuration of PV/PCM system and type – B configuration of PV/PCM system. Figure 5.13 also depicts the evolution of total utilized radiation with extension ratio for type – B configuration ($L_1/L = 0.3$). Conventional PV system without any PCM enclosure utilize incoming radiation in form of electric power only. Initially, PV panel absorbs 101.66 W/m^2 of incoming radiation which decreases to 86.78 W/m^2 with progression of time due to increased PV cell temperature. Most of the radiation is lost to surroundings and PV system is

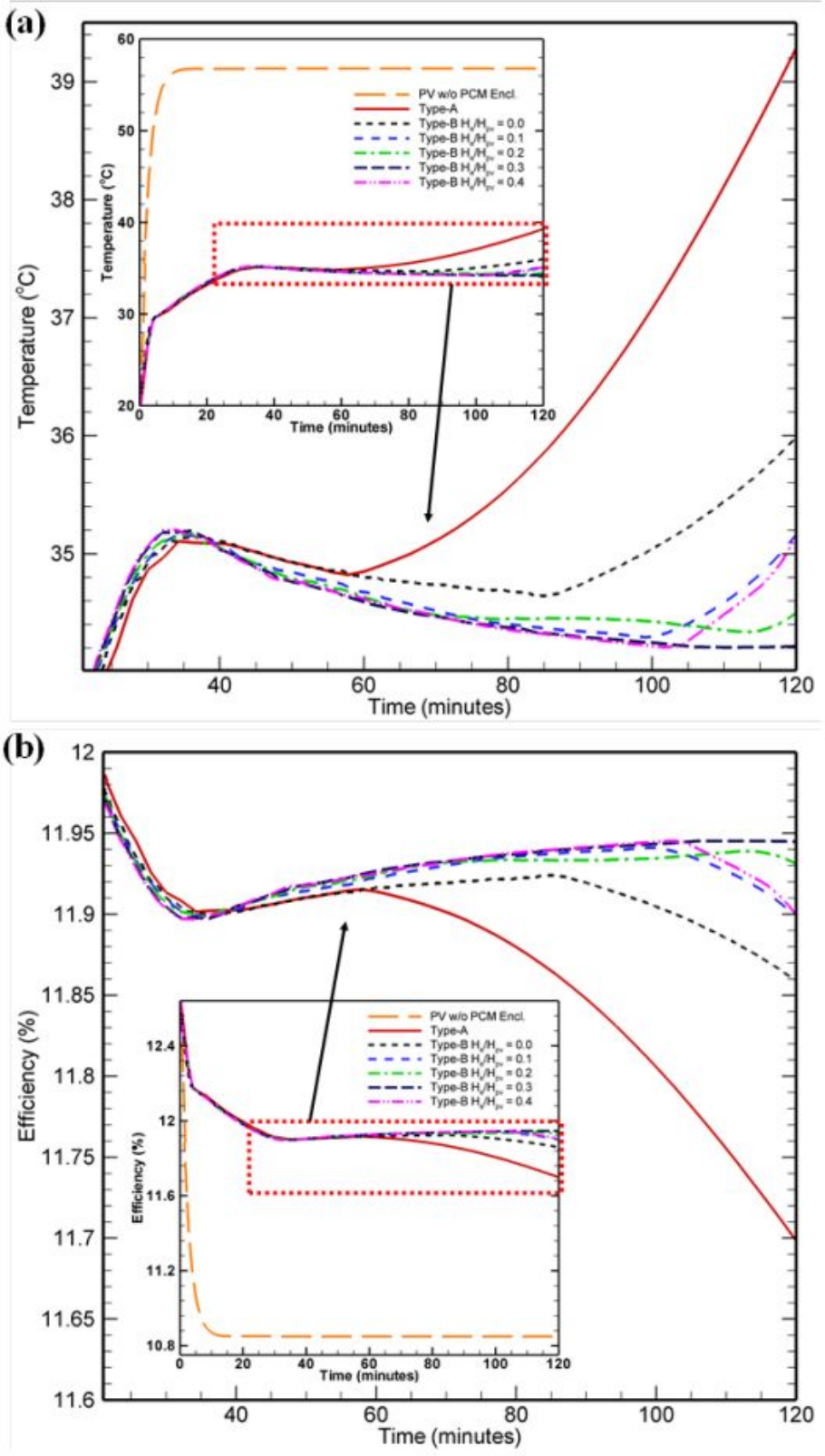

Figure 5.11: Transient variation of (a) PV cell temperature (b) PV cell electric conversion efficiency for type – B configuration of PV/PCM system at lower thickness ratio (L_1/L = 0.3). Full transient history are shown in inset for each curve.

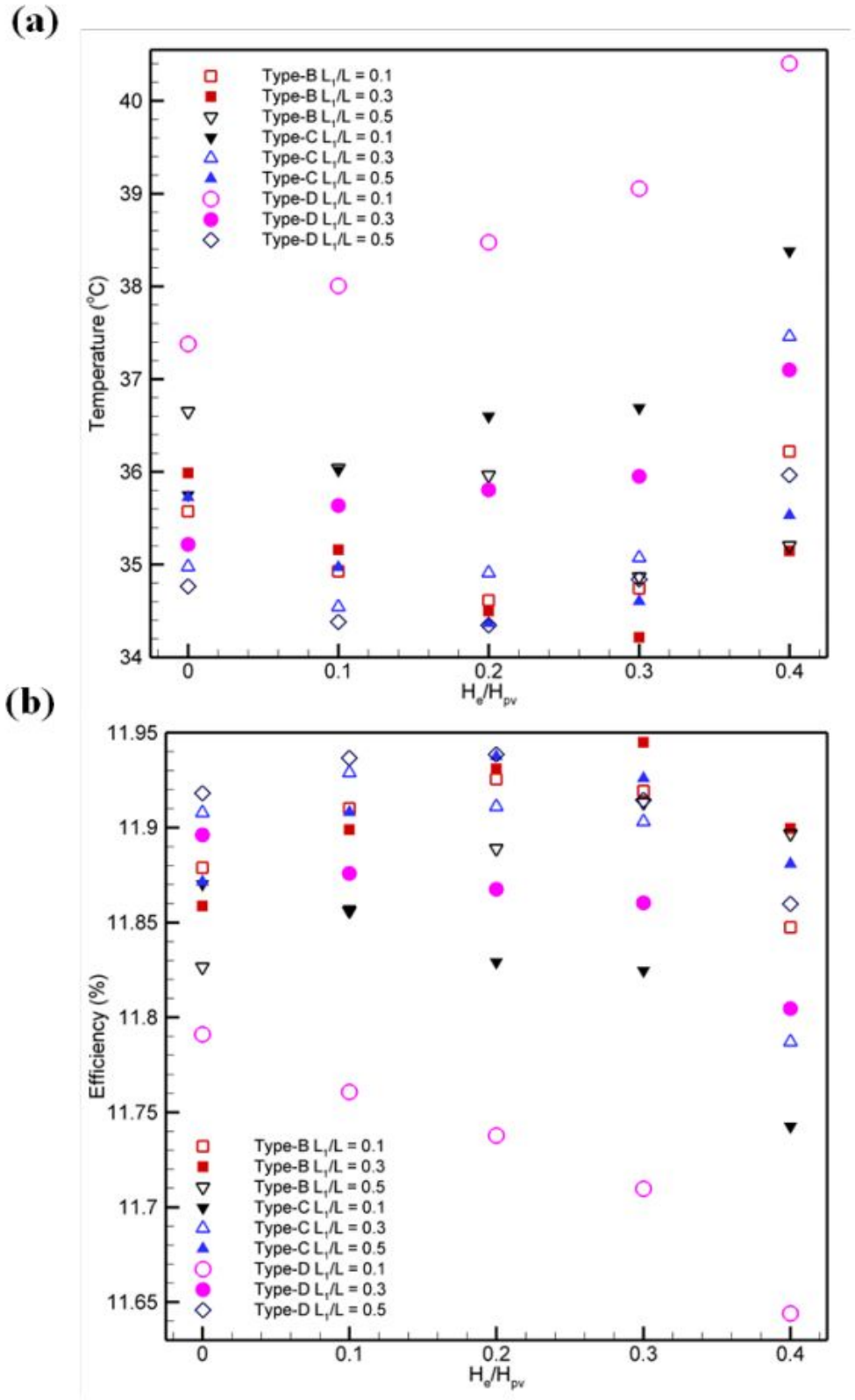

Figure 5.12: Comparison of (a) PV cell temperature, and (b) PV cell electric conversion efficiency at 120 minutes of process among all configuration of PV/PCM system with non-rectangular PCM enclosure.

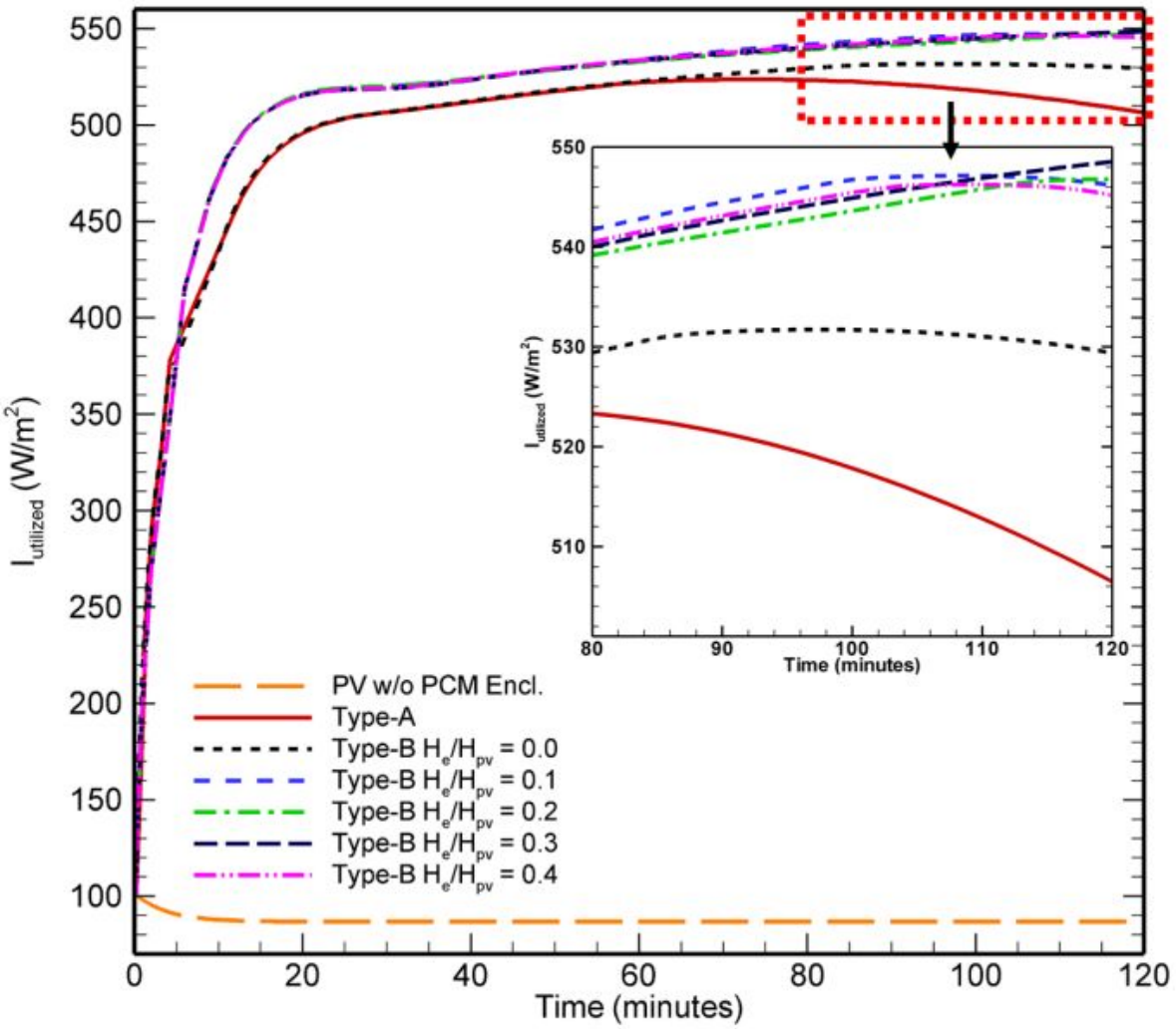

Figure 5.13: Transient variation of total utilized radiation for type – B configuration of PV/PCM system at lower thickness ratio ($L_1/L = 0.3$). Expanded view of selected part of curve is shown in inset.

able to use only 10.84% of incoming radiation which is very low. Addition of PCM enclosure to PV system increases the radiation absorption capacity of the system as it store radiation in form of heat and also increase electric power by reducing operating temperature of PV panel. For type – A configuration of PV/PCM system, total utilized radiation has increased to 506.47 W/m^2 by the end of 120 minutes which is 63.31% of incident radiation. Electric power generation has also increased to 93.52 W/m^2 by 120 minutes as a result of temperature reduction which is a significant improvement. Further, the use of type – B configuration ($H_e/H_{pv} = 0.0, L_1/L = 0.3$) of PV/PCM system has increased total utilized radiation to 529.38 W/m^2 (66.17% of incoming radiation with 94.88 W/m^2 of electric power generation. The utilized radiation first increases with extension ratio up to optimum extension ratio and then starts decreasing for type – B configuration ($L_1/L = 0.3$) of PV/PCM system. The optimum extension ratio for this configuration is 0.3

and total utilized radiation has reached to a maximum value of 548.54 W/m^2 (68.56% of incoming radiation) with electric power generation capacity of 95.64 W/m^2 by the end of 120 minutes. Further effect of extension ratio and lower thickness ratio on total utilized radiation for all type of configurations of PV/PCM system is given in Figure 5.14. It is not necessary that performance of PV/PCM system increases on using extended PCM enclosure, it may decrease depending on distribution of mass with in the enclosure. Type – C configuration ($L_1/L = 0.1$) and type – D configuration ($L_1/L = 0.1\&0.3$) exhibit continuous degradation in radiation utilizing ability of the system with rise of extension ratio. However, type – C configuration exhibit an optimum extension ratio of 0.1 at $L_1/L = 0.3$ and 0.2 at $L_1/L = 0.5$) respectively. Type – C configuration ($L_1/L = 0.5$) exhibit a maximum value of utilized radiation of 547.08 W/m^2 (68.38% of incoming radition) at optimum extension ratio of 0.2. Type – D configuration ($L_1/L = 0.5$) also exhibit an optimum extension ratio 0.2 at which its maximum utilization radiation of 547.15 W/m^2 (68.38% of incoming radition). Type – B configuration exhibit three different value of optimum extension ratio of 0.2 at $L_1/L = 0.1$ and 0.3 at at $L_1/L = 0.3$ & 0.5 respectively. The optimum extension ratio is different for different configurations at different values of lower thickness ratio. This is due to the fact that these parameters decides distribution of mass with in the PCM enclosure and optimum extension ratio ensures the maximum availability of PCM for convection dominated melting for maximum duration. Though, type – C & D configuration ($H_e/H_{pv} = 0.2, L_1/L = 0.5$) exhibit approximately similar performance to type – B configuration ($H_e/H_{pv} = 0.3, L_1/L = 0.3$) but still type – B configuration is recommended due to more compactness and simplified geometry.

Overall performance of the system can also be analyzed by estimating the ratio of utilized radiation to unutilized radiation ($I_{gain} = I_{utilised}/I_{unutilised}$). The I_gain ratio reflects the radiation management ability of the system i.e how much radiation is utilized per unit loss of incoming radiation. The transient variation of I_{gain} ratio at different extension ratios for type - B configuration is shown in Figure 5.15 and compared to type – A configuration and no PCM enclosure configuration of systems.

Conventional PV system exhibit very low value of I_{gain} ratio as most of the incoming radiation lost to surroundings. For all type of PV/PCM systems, the value of I_{gain} ratio starts to increase with increase in absorbed radiation with progression of time. Initial value of I_{gain} ratio is not zero as electrical power contributes to utilized radiation, however it is of very low value as most of radiation is lost to surrounding in form of heat.

The slope of I_{gain} ratio – time curve is steeper in conduction regime due to rapid absorption of latent heat initially. The curve become flatter in mixed regime and I_{gain} ratio starts to increase in quasi-convection regime with development of convection current in liquid PCM region. The I_{gain} ratio approaches to maximum value at the end of convection regime and starts to decrease with time in solid shrinking regime. This maximum point for type – A configuration occurs at only 56 minutes and as consequence it exhibit I_{gain} ratio of value 1.72 at end of

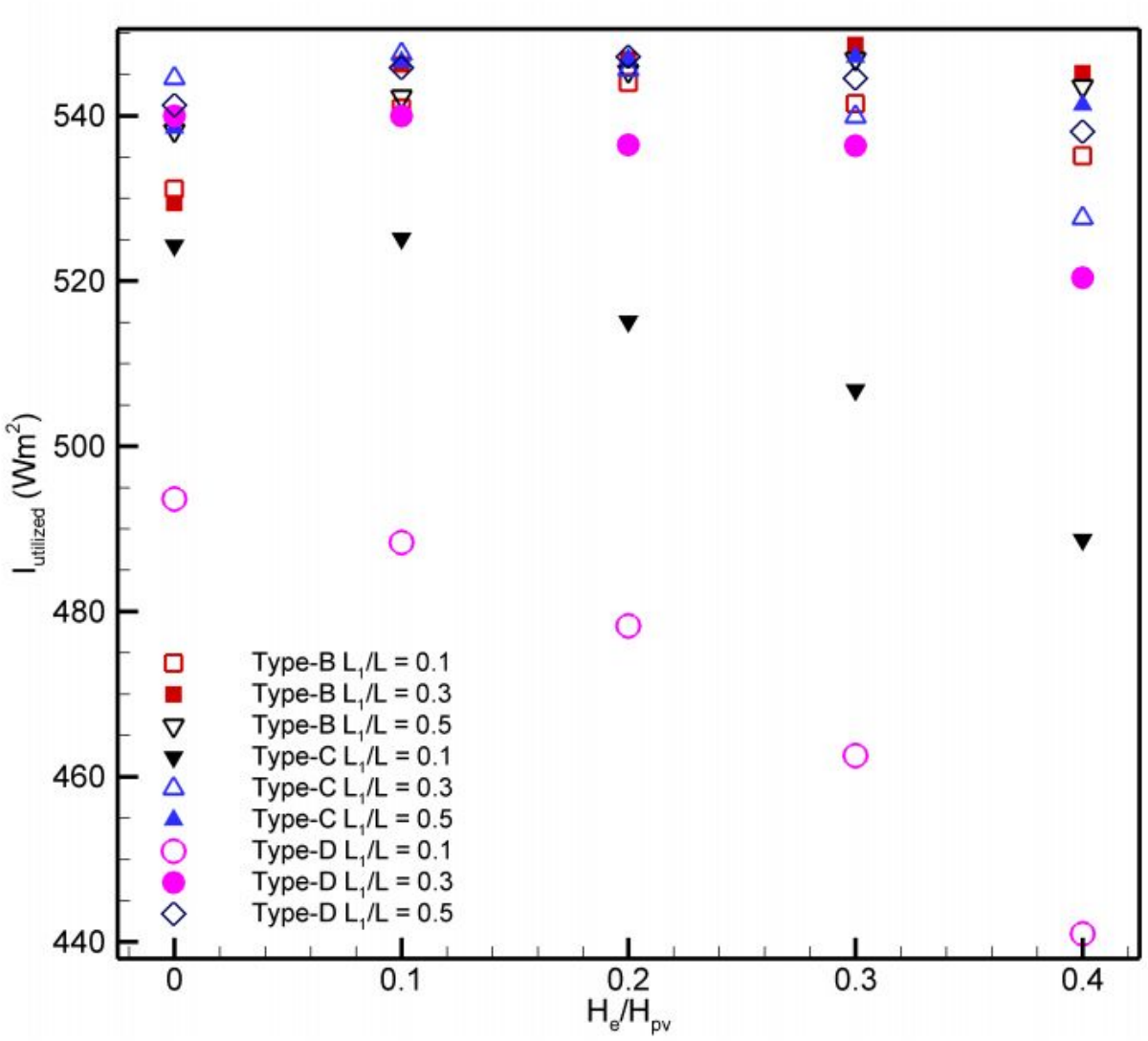

Figure 5.14: Comparison of total utilized radiation at 120 minutes of process among all configuration of PV/PCM system with non-rectangular PCM enclosure.

120 minutes. In Type – B configuration ($H_e/H_{pv} = 0.0, L_1/L = 0.3$), I_{gain} ratio increases to 1.96 due to a longer convection regime of 84 minutes. With increase in extension ratio, duration of convection dominated melting increases, hence I_{gain} ratio increases with extension ratio till an optimum extension ratio and after that it decreases. For type – B configuration($L_1/L = 0.3$), the optimum extension ratio is found to be 0.3 where it exhibit a maximum I_{gain} ratio of 2.18. This indicates that system absorbed radiation is 2.18 times of lost radiation. Type – B configuration ($H_e/H_{pv} = 0.3, L_1/L = 0.3$), exhibit an improvement of 26.74 % compared to type – A configuration and 11.22% compared to type – B configuration ($H_e/H_{pv} = 0.0, L_1/L = 0.3$) in radiation management ability of the system.

Figure 5.16 shows the comparison of I_{gain} ratio and its variation with extension ratio and lower thickness ratio for all configurations of PV/PCM system. The I_{gain} ratio exhibit the similar

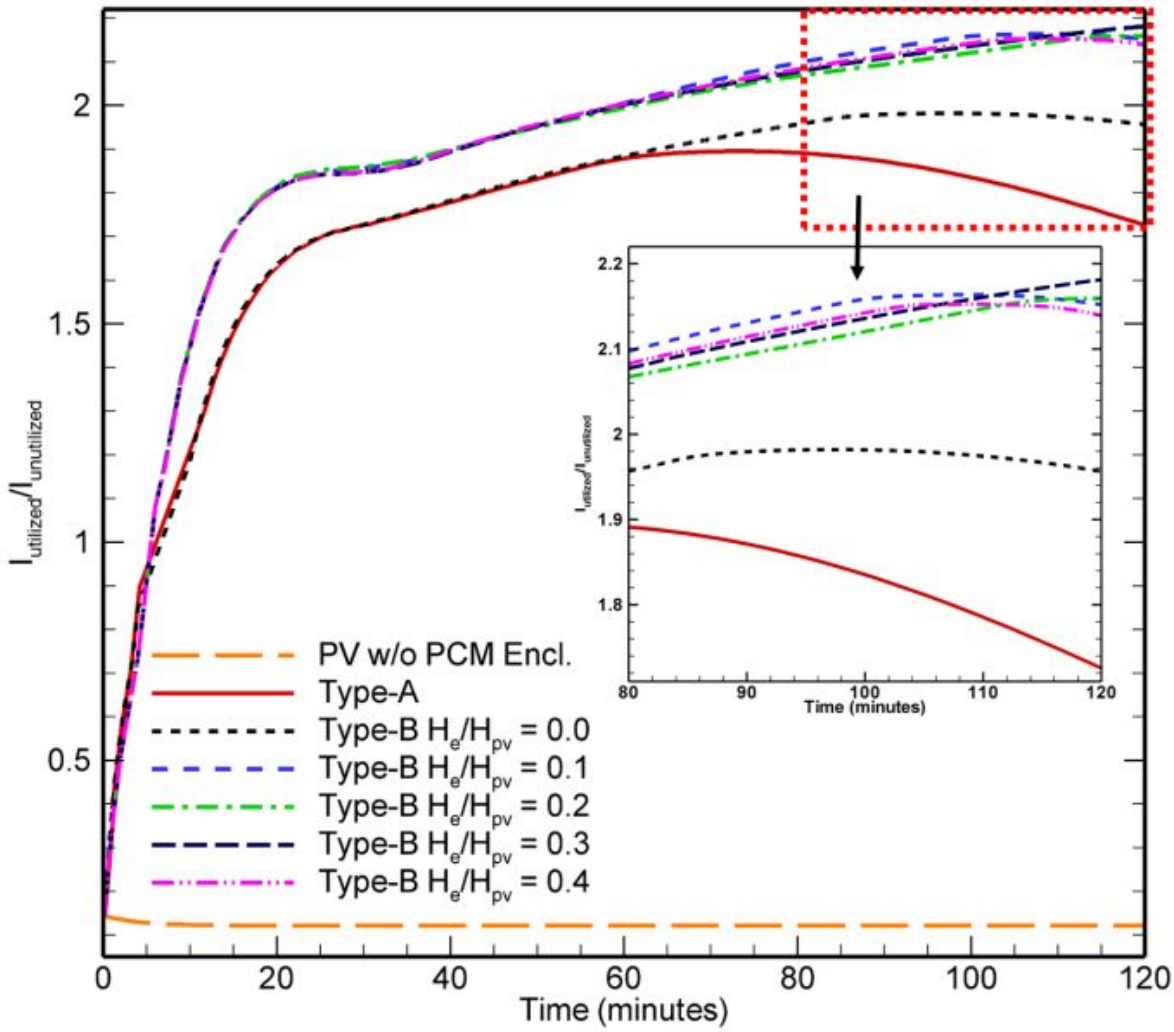

Figure 5.15: Transient variation of I_{gain} ratio for type – B configuration of PV/PCM system at lower thickness ratio ($L_1/L = 0.3$). Expanded view of selected part of curve is shown in inset.

trend with extension ratio as total utilized radiation exhibited for all configurations. Both type – C &D configuration exhibit maximum value of I_{gain} ratio of 2.16 at optimum extension ratio of 0.2 and lower thickness ratio of 0.5, which is 4.98% and 3.45% improvement compared to their respective non-extended counterpart. Type – B configuration ($H_e/H_{pv} = 0.3, L_1/L = 0.3$) has not only shown marginally enhanced improvement in I_{gain} ratio compared to type – C & D configuration ($H_e/H_{pv} = 0.2, L_1/L = 0.5$) but it is also more compact and possess a simplified geometry to manufacture. Therefore, it is recommended for better overall performance of PV/PCM system.

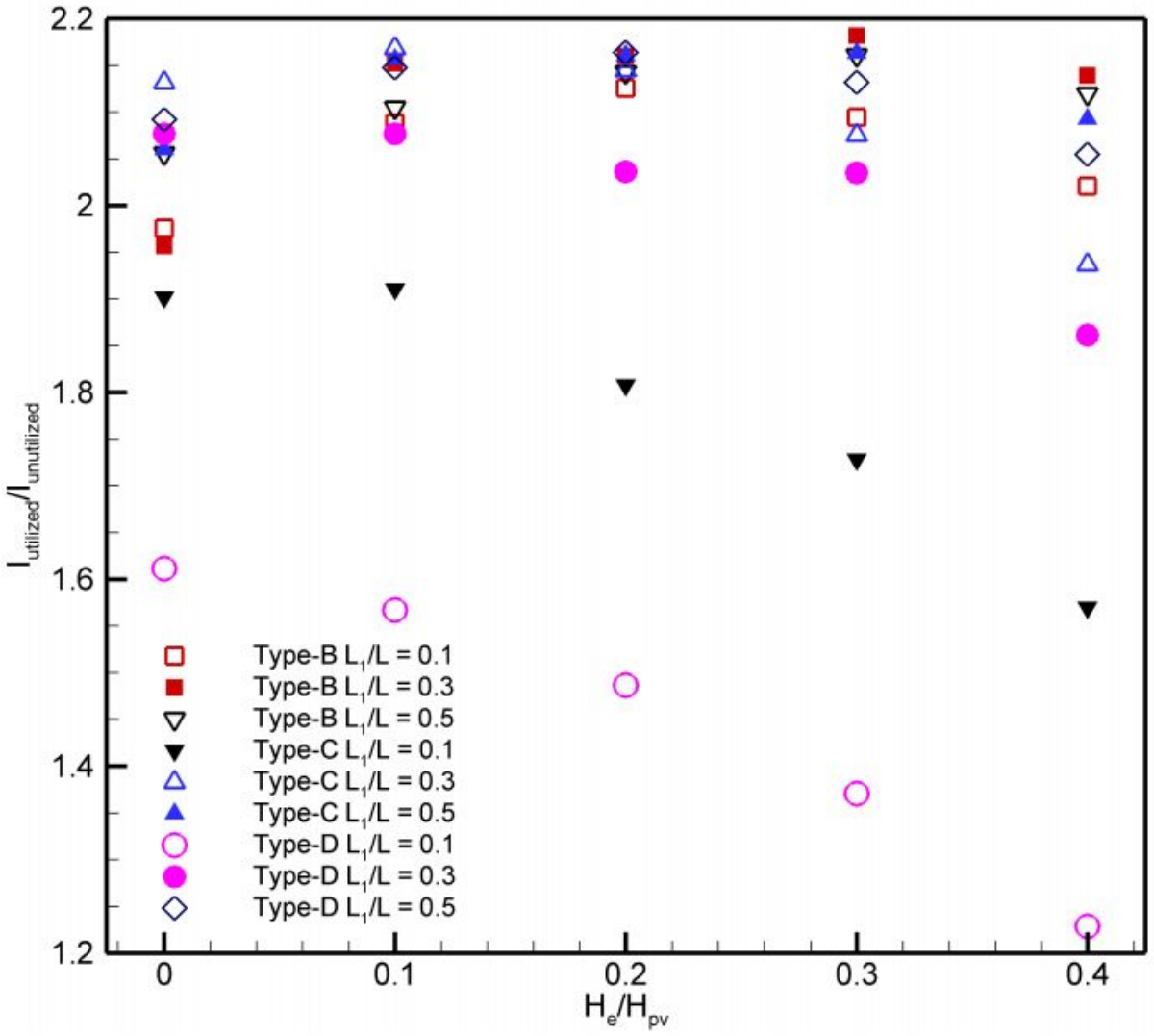

Figure 5.16: Comparison of I_{gain} ratio at 120 minutes of process among all configuration of PV/PCM system with non-rectangular PCM enclosure.

5.4 Conclusions

In this chapter, new extended non-rectangular designs of PCM enclosures has been proposed to promote the enhancement in thermo-electric performance and incoming radiation utilization ability of PV/PCM system. An experimental validated computational model is developed to analyze melting morphology and its effect on thermo-electric performance of the system. The evolution of design of non-rectangular enclosures are done on basis of certain geometrical parameters such as profile of right wall, lower thickness ratio (L_1/L), and extension ratio (H_e/H_{pv}) to enhance the span of convection driven melting. These geometrical parameters affects the PCM distribution with in the enclosure and also decides the compactness of the system. The non-rectangular PCM enclosure has the same volume as rectangular enclosure (type – A). Non-

rectangular enclosure are designated as type – B, C, & D for linear, parabolic, & cubic right wall profile respectively. The optimum extension ratio and lower thickness ratio are found according to melting front morphology, and thermos-electric performance after many design iterations. Melting behavior, energy storage density, electric conversion efficiency, total utilized radiation and I_{gain} ratio are reported in detail. Some important outcomes are as follows:

1. Type – B configuration ($H_e/H_{pv} = 0.3, L_1/L = 0.3$), exhibit prolonged span of quasiconvection regime (120 minutes) due to which convective heat transfer is dominant in enclosure (Nu is enhanced by 66.87%) and 20.5% more melting is achieved compared to type – A configuration of PV/PCM system.

2. Electric conversion efficiency approaches to 96.37 % of its rated value which was 87.41% for simple PV system and 94.27% for type – A configuration of PV/PCM system. This enhancement is due to reduction of 22.57°C in PV cell temperature compared to simple PV system.

3. The ability to utilized incoming radiation has been increased to 67.35% with a total utilized radiation of 538.76 W/m^2 in Type – B configuration ($H_e/H_{pv} = 0.3, L_1/L = 0.3$) which was just 61.61% (492.09 W/m^2) in type – A configuration of PV/PCM system.

4. Enhanced I_{gain} ratio (2.18) suggest that Type – B configuration ($H_e/H_{pv} = 0.3, L_1/L = 0.3$) system has better incoming radiation management ability than any other discussed configuration.

Type – B configuration ($H_e/H_{pv} = 0.3, L_1/L = 0.3$) is recommended for not only exhibit maximum thermo-electric performance but for also most compact structure among all good performing configurations. This research would assist research community in developing energy efficient designs of PCM enclosures for PV/PCM system so that ever-rising energy demand could be meet by producing extra electric power and storing remaining radiation in form of heat for later usage.